

REPORT

ON A

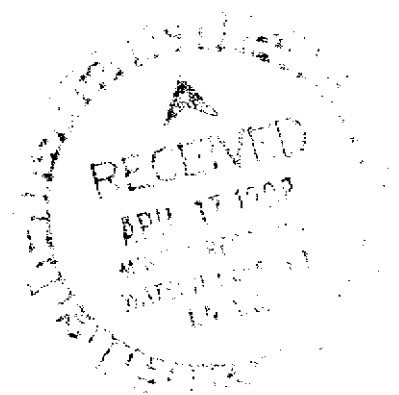
**COMBINED HELICOPTER-BORNE
ELECTROMAGNETIC, MAGNETOMETER and VLF-EM
JOINT AERODAT SURVEY
WOLF DEPOSIT AND NEARBY BELT
YUKON TERRITORY**

FOR

**PATHFINDER RESOURCES LTD.
COMINICO LTD.
ATNA RESOURCES LTD.
YGC RESOURCES LTD.**

BY

**HIGH-SENSE GEOPHYSICS LTD.
47 Jefferson Ave.
Toronto, Ontario
Canada, M6K 1Y3**



Voice: +1 416 588-7075

Fax: +1 416 588-9789

Bob Lo, M.Sc., MBA, P. Eng.
Consulting Geophysicist

This report has been examined by
the Geological Evaluation Unit
under Section 53 (4) Yukon Quartz
Mining Act and is allowed as
representation work in the amount
of \$ 14,000.

M.B.H.
for Regional Manager, Exploration and
Geological Services for Commissioner,
of Yukon Territory.

TABLE OF CONTENTS

SUMMARY	1
1. INTRODUCTION	1
2. LOCATION, ACCESS AND TOPOGRAPHY	1
3. SURVEY PROCEDURES AND THE PHYSICAL SURVEY	3
3.1 SURVEY PROCEDURES	3
3.2 THE PHYSICAL SURVEY	3
4. DELIVERABLES	4
5. AIRCRAFT AND EQUIPMENT	4
5.1 AIRCRAFT	4
5.2 ELECTROMAGNETIC SYSTEM	4
5.3 MAGNETOMETER	5
5.5 IN-FIELD PROCESSING	5
5.6 ANCILLARY SYSTEMS	5
BASE STATION MAGNETOMETER	5
RADAR ALTIMETER	6
TRACKING CAMERA	6
GPS NAVIGATION SYSTEM	6
ANALOGUE RECORDER	6
DIGITAL RECORDER	7
5.7 EQUIPMENT RACK AND INSTALLATION	7
6. DATA PROCESSING AND PRESENTATION	8
6.1 IN-FIELD PROCESSING	8
6.2 BASE MAP	8
6.3 FLIGHT PATH MAP	8
6.4 DIGITAL ELEVATION MODEL	9
6.5 ELECTROMAGNETIC SURVEY DATA	9

APPARENT CONDUCTIVITY	10
6.6 MAGNETIC DATA	10
TOTAL MAGNETIC INTENSITY	10
CALCULATED VERTICAL MAGNETIC GRADIENT	10
COLOUR SHADOW MAP	10
6.8 EM ANOMALY SELECTION AND ANALYSIS	11
ANOMALY SELECTION	11
ANALYSIS	12
7. GEOLOGY	12
7.1 PROJECT GEOLOGY AND TARGETS	12
8. INTERPRETATION	13
8.1 GEOLOGIC INTERPRETATION	13
8.2 ELECTROMAGNETIC INTERPRETATION	16
8.3 AREAS OF INTEREST	16
9. CONCLUSIONS AND RECOMMENDATIONS	20
REFERENCES	21

LIST OF APPENDICES

APPENDIX 1 -	Personnel
APPENDIX 2 -	General Interpretive Considerations
APPENDIX 3 -	Anomaly Listings
APPENDIX 4 -	Statement of Qualifications
APPENDIX 5 -	Statement of Expenditures (Cominco Ltd.)

LIST OF FIGURES

FIGURE 1	-	General Location Map
FIGURE 2	-	Claim Map
FIGURE 3	-	EM Interpretation and Total Field Magnetics

SUMMARY

A helicopterborne electromagnetic and magnetic survey was conducted over the Wolf Deposit and nearby belt in southern Yukon Territory, Canada. The survey was jointly conducted for Pathfinder Resources Ltd., Cominco Ltd., Atna Resources Ltd., and YGC Resources Ltd. Total survey coverage is 998 kilometres (908 km survey lines and 90 km tie lines).

The data collected is of use in mapping the geology of the survey area and in delineating areas consistent with the primary targets being sought. The primary targets are Kuroko type VMS mineralisation. They are relatively easy geophysical targets as they are conductive and may be directly detectable with the electromagnetic system. However, the EM responses in area may be due to a myriad of other sources such as the black shales. The magnetics is of use to search for areas of alteration (magnetite destruction) and as a mapping tool. Forty-six targets are located with fifteen targets of high priority which should be followed up first.

Follow up work may start by prospecting of the top ranked anomalies. Ground magnetometer and VLF surveys may be sufficient for geophysical ground follow up, but horizontal loop EM is a more certain EM technique if the prospecting confirms that the targets are in favourable settings or if prospecting can not find the source of the anomalies. Correlation with known geology and geochemistry should be done to reassess the geophysical anomalies as the interpreted setting was used to weigh the anomalies.

Depending on the results, the most favourable of the targets should be considered for drill testing.

**REPORT ON A
COMBINED HELICOPTER-BORNE
ELECTROMAGNETIC, MAGNETOMETER and VLF-EM
JOINT AERODAT SURVEY
WOLF DEPOSIT AND NEARBY BELT
YUKON TERRITORY**

1. INTRODUCTION

A joint helicopter-borne electromagnetic (EM), magnetometer and VLF-EM survey was flown over the Wolf Deposit and nearby belt in southern Yukon Territory by Aerodat. The participants in the joint survey were Pathfinder Resources Ltd., Cominco Ltd., Atna Resources Ltd., and YGC Resources Ltd. The survey was flown as part of an on-going effort to delineate areas of favourable mineralisation in the vicinity of the Wolf Deposit and nearby belt.

The primary targets are envisaged to be the Kuroko type of VMS deposits similar to the Wolf Deposit and perhaps gold deposits similar to the Ketzka River Deposit. The massive sulphides of the VMS targets should be directly detectable by the EM methods if they occur sufficiently close to the surface. However, other EM responses such as those from the black shales of the area can mimic the conductive response of the VMS. The acquisition of magnetometer data was used as a mapping tool. The magnetometer data is also used to search for magnetic intrusives and perhaps for areas of magnetite destruction caused by alteration.

The survey was flown between October 27, and November 10, 1997. Twenty-four flights were required to complete the survey. The base of operations was at Ross River, some 80 kilometres to the north northwest. Survey lines were spaced 200 metres apart and oriented at 40° and 220° azimuth. Tie lines were flown at 2,000 metre intervals in a direction orthogonal to the survey lines.

Total survey coverage is 998 kilometres. This is distributed as 908 km and 90 km of survey and tie lines respectively. Aerodat's internal reference for this contract is J9795.

Between the time of the data collection in the Yukon, and the completion of this report, Aerodat Inc. was placed into receivership. Subsequently, High-Sense Geophysics Ltd. purchased the assets and then contracted GCT Consulting Services of Toronto (416 694-6974) to complete the processing and reporting.

2. LOCATION, ACCESS AND TOPOGRAPHY

The survey area is located in southern Yukon Territory, some 80 kilometres south, southeast of Ross River and is shown on the attached index map that includes geographic references and coordinates. An index map also appears on all map products. The centre of the survey is located at approximately 61° 15' N and 131° 25' W.

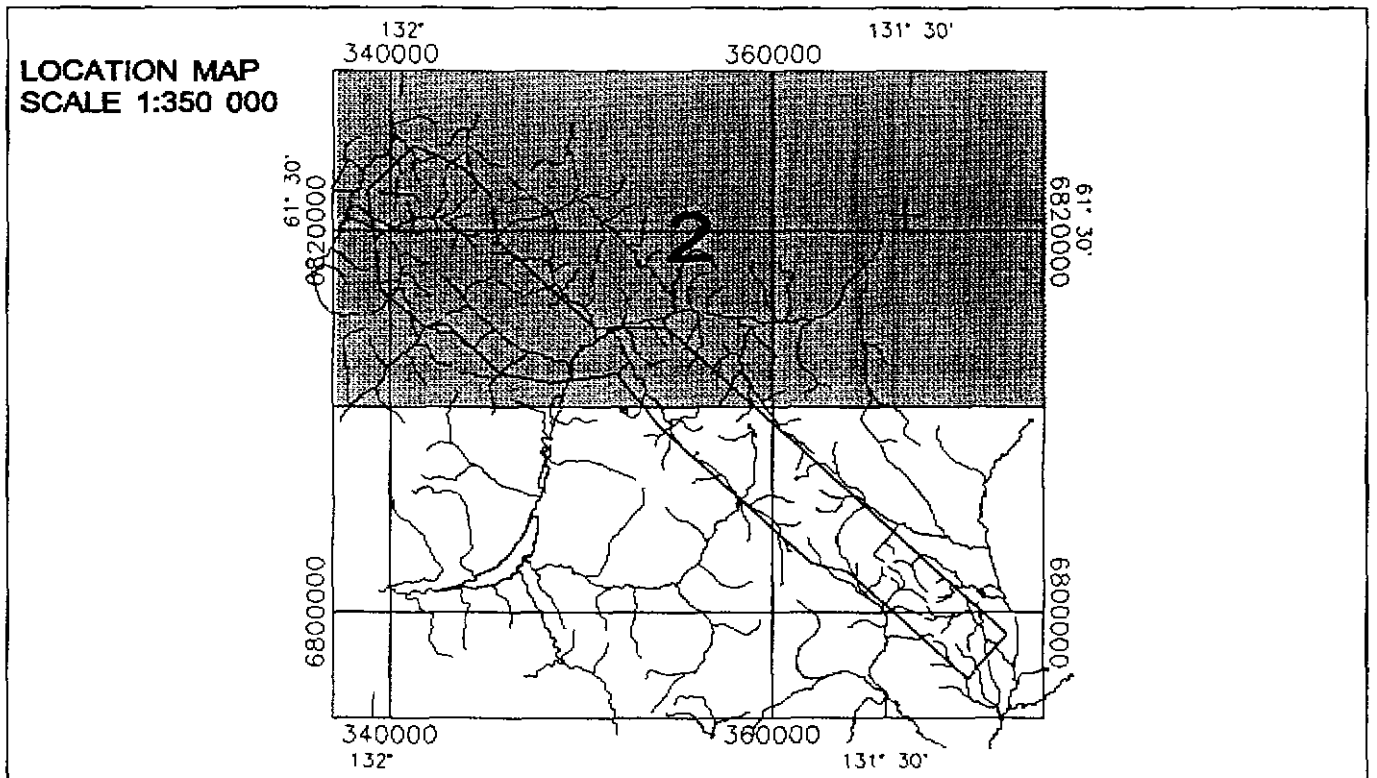
Access to the property at the north end of the survey is provided by the Ketz River Mine road some five kilometres to the northwest. In the southern part of the survey area, access to the Wolf Deposit is provided by a cat trail from the Robert Campbell Highway.

The topography of the area is rugged with an elevation variation of between 1200 metres to just over 2,000 metres above sea-level. Steeply incised drainages and steep slopes are interspersed with wide valley floors around over the survey area.

The survey boundary is defined by the following points:

Easting	Northing	Easting	Northing
370214	6796486	339514	6816986
363914	6802186	338814	6822236
362014	6802586	341214	6824586
354114	6809786	343714	6823486
351914	6812586	345314	6821986
348414	6812086	345614	6819586
345814	6812586	350714	6814986
342914	6815186	354514	6814986
341814	6814986	372314	6798836

Table 1, Survey boundary coordinates (UTM coordinates)



INDEX MAP: Joint Aerodat Survey, Wolf Deposit and nearby Belt

3. SURVEY PROCEDURES AND THE PHYSICAL SURVEY

3.1 Survey Procedures

Aircraft ground speed is maintained at approximately 60 knots (30 metres per second). An aircraft terrain clearance of 60 metres, which is consistent with the safety of the aircraft and crew, was attempted.

A global positioning system (GPS) consisting of a Magnavox MX 9212 assists in aircraft navigation and flight line control. The receiver antenna is mounted on the magnetometer bird. A base station is used to record static positions for the removal of Selective Availability (a signal degradation technique used by the military to deny the full accuracy of GPS to unauthorised users) from the readings of the helicopter GPS. The base station GPS was located at the base of operations in Ross River, away from cultural effects. Differential processing of the GPS data in the field and in the Mississauga office utilises a PC using software supplied by the manufacturer.

Pathfinder Resources Ltd. provided the UTM coordinates of the survey area corners. These coordinates are programmed into the navigation system along with the survey grid. As a check, the operator enters manual fiducials over prominent topographic features. These manual fiducials are a confirmation of the electronic navigation when plotted on topography maps. Survey lines showing excessive deviation as determined by the in-field processing are re-flown.

Aircraft position is registered by the navigation system. The operator calibrates the geophysical systems at the start, middle (if required) and end of every survey flight. During calibration the aircraft is flown away from ground effects to record electromagnetic zero levels.

In-field processing consisting of data verification, and backups and some raw outputs was conducted using a Pentium based PC and Geosoft software. Differentially corrected flight paths, raw magnetometer, mid frequency coaxial and coplanar EM data, and radar altimeter were outputted in the field. A colour dot matrix printer/plotter was used as the output device.

3.2 The Physical Survey

The survey was flown between October 27, and November 10, 1997. Twenty-four flights were required to complete the survey. The base of operations was at Ross River, some 80 kilometres to the north northwest. At the base of operations, the in-field processing, base station magnetometer, and base station GPS were set up.

Survey lines were spaced 200 metres apart and oriented at 40° and 220° azimuth. Tie lines were flown at 2,000 metre intervals in a direction orthogonal to the survey lines.

The VLF-EM stations which were used were a combination of Cutler, Seattle, and Annapolis.

4. DELIVERABLES

The maps and report on the results of the survey are presented in three copies. The report includes folded white print copies of the 1:20,000 scale interpretation maps. Three copies of the colour, and colour shadow maps are in an accompanying map tube. The colour maps have a digitised planimetry, plus the UTM grid coordinates and the survey boundary for reference.

The UTM projections are in the North American Datum of 1927 coordinate system which uses the Clarke 1866 spheroid and local datum shifts of $dx = -10$, $dy = 158$, $dz = 187$. A central meridian of 129° West was used for the UTM projections.

The processed digital data, including both the profile and the gridded data, is on CD ROMs (ISO 9660). Profile data is written as columnar ASCII records and the gridded data as standard Geosoft PC grids. A full description of the format is included with the package. All gridded data can be displayed on PCs using the Aerodat AXIS (Aerodat Extended Imaging System) or, via grid conversions, on other imaging software. The complete data package includes all analogue records, base station magnetometer records, and flight path video tape.

5. AIRCRAFT AND EQUIPMENT

5.1 Aircraft

An Aerospatiale AS350B1 (Ecureil) helicopter with Canadian registration C-GKHS owned and operated by Kluane Helicopters was used for the survey. Geophysical and ancillary equipment was installed by Aerodat. The pilot for the surveys was Bill Karman from Kluane Helicopters. Where possible during surveys, the survey aircraft flies at a mean terrain clearance of 60 metres (200 feet) and speed of 60 knots.

5.2 Electromagnetic System

The electromagnetic system is an Aerodat five frequency configuration. The transmitter and receiver coils and electronics are mounted in a rigid kevlar shell termed an EM bird. The survey was flown with the Aerodat bird designated Kestrel. Two vertical coaxial coil pairs and three horizontal coplanar coil pairs are operated at the frequencies and coil separations described below.

	Coaxial 1	Coaxial 2	Coplanar 1	Coplanar 2	Coplanar 3
Frequency (Hz)	912	4,365	861	4,765	33,020
Coil Spacing (m)	6.4	6.4	6.4	6.4	6.4

Inphase and quadrature signals are measured simultaneously for the five frequencies with a time constant of 0.1 seconds. System noise levels are generally less than one ppm excluding spherics. Digital despiking and filtering of the EM signals permit rejection of the spheric noise to less than one ppm. The HEM bird is towed 30 metres below the helicopter.

5.3 Magnetometer

An optically pumped cesium vapour magnetometer sensor manufactured by Scintrex, coupled to a proprietary magnetometer console designed by Aerodat measures the Earth's magnetic field. The sensitivity of this instrument is 0.001 nanoTesla at a sampling rate of 0.1 second. The sensor is towed in a bird 15 metres below the helicopter, nominally 45 metres above the surface.

5.5 In-field Processing

The infield processing unit consisted of an Pentium class PC with the proper tape drives and backup devices to read and backup the data collected during flight. A colour monitor and a colour dot matrix printer/printer was used. Software was Geosoft's Geophysical Processing and Presentation software.

During the survey, in-field processing verified that the data were recorded properly and that the noise specifications were adhered to. Data integrity was ensured via backups. Processing of data using Aerodat and Geosoft software recovered the GPS flight path and performed the differential corrections. Plots of the flight path and raw magnetometer and total count were outputted to determine if the data were within contractual specifications.

5.6 Ancillary Systems

Base Station Magnetometer

A second Scintrex magnetometer sensor and Aerodat console is set up at the base of operations to record temporal variations of the earth's magnetic field. Synchronization of the base station magnetometer's clock with that of the airborne system is done to facilitate later correlation. Recording resolution is 0.01 nT with an update rate of one second. Magnetic field variation data are recorded both digitally and on printer plots. The date and chart settings are given at the start of the hard copy record.

Radar Altimeter

A King KRA-10A radar altimeter was used to record the terrain clearance. The output from the instrument is a linear function of altitude. The altimeter is mounted on the helicopter.

Tracking Camera

A Sony colour video camera records the flight path on VHS video tape. The camera operates in continuous mode. The video tape also shows the flight number, 24 hour clock time (to .01 second), and manual fiducial number.

GPS Navigation System

The GPS navigation system in the helicopter consists of a Magnavox MX 9212 with a NavPilot navigation console and a notebook computer to record data. Position information from the airborne GPS receiver is recorded on disk at an update rate of 1.0 seconds. The survey lines are programmed into the navigation console, which receives position information from the airborne receiver and provides left/right guidance information to the pilot. On the ground, a Novatel 3151R GPS receiver and notebook computer datalogger is used to log data for post-flight differential correction of airborne data.

Analogue Recorder

An RMS dot matrix recorder displays the data during the survey. This allows the geophysical operator to scan the data as it is collected to ensure that the system is functioning properly. As the analogue recorder records the raw output of the instrumentation, it is used for visual inspection of the system noise. Record contents are as follows:

LABEL	PARAMETER	CHART SCALE
GEOPHYSICAL SENSOR DATA		
MAGF	Total Magnetic Intensity, Fine	2.5 nT/mm
MAGC	Total Magnetic Intensity, Coarse	25 nT/mm
L9XI	912 Hz, Coaxial, Inphase	2.5 ppm/mm
L9XQ	912 Hz, Coaxial, Quadrature	2.5 ppm/mm
M4XI	4,365 Hz, Coaxial, Inphase	2.5 ppm/mm
M4XQ	4,365 Hz, Coaxial, Quadrature	2.5 ppm/mm
L8PI	861 Hz, Coplanar, Inphase	10 ppm/mm
L8PQ	861 Hz, Coplanar, Quadrature	10 ppm/mm
M4PI	4,765 Hz, Coplanar, Inphase	10 ppm/mm
M4PQ	4,765 Hz, Coplanar, Quadrature	10 ppm/mm
H3PI	33,020 Hz, Coplanar, Inphase	20 ppm/mm
H3PQ	33,020 Hz, Coplanar, Quadrature	20 ppm/mm
VLT	VLF-EM, line station, Total Field	2.5%/mm
VLQ	VLF-EM, line station, Quadrature	2.5%/mm

VOT	VLF-EM, Ortho station, Total Field	2.5%/mm
VOQ	VLF-EM, Ortho station, Quadrature	2.5%/mm

ANCILLARY DATA

RALT	Radar Altimeter	10 ft/mm
BALT	Barometer	50 ft/mm
GALT	GPS Altimeter	50 ft/mm
PWRL	60/50 Hz Power Line Monitor	-
VREF	Voltage Reference	-

The zero level of the radar altimeter is 5 cm from the top of the analogue record. A helicopter terrain clearance of 60 m (200 feet) should therefore be seen some 3 cm from the top of the analogue record.

Chart speed is 2 mm/second. The 24 hour clock time is printed every 20 seconds. The total magnetic field value is printed every 30 seconds. The ranges from the radar, and navigation system are printed every minute.

Vertical lines crossing the record are manual fiducial markers activated by the operator. The start of any survey line is identified by two closely spaced manual fiducials. The end of any survey line is identified by three closely spaced manual fiducials. Manual fiducials are numbered in order. Every tenth manual fiducial is indicated by its number, printed at the bottom of the record. Background calibration sequences are present at the start and end of each flight and at intermediate times where needed.

Digital Recorder

A DGR-33 data acquisition system digitises and records the survey data on magnetic media. Contents and update rates are as follows:

DATA TYPE	SAMPLING RATE	RESOLUTION
Magnetometer	0.1 s	0.001 nT
HEM, coaxial - 912 / 4,365 Hz	0.1 s	0.03 ppm
HEM, coplanar - 861 / 4,765 Hz	0.1 s	0.06 ppm
HEM, coplanar - 33,020 Hz	0.1 s	0.125 ppm
VLF-EM (4 Channels)	0.2 s	0.01%
Position (3 Channels)	0.1 s	0.1 m
Altimeter (2 Channels)	0.2 second	0.05 m
Power Line Monitor	0.2 second	
Manual Fiducial		
Clock Time		

5.7 Equipment Rack and Installation

The power supply and the data acquisition system is mounted on a standard 19 inch equipment rack which is mounted in a floor board and secured to the helicopter. Cables are run through the helicopter to connect on to the tow cable outside. The

tow cable supports the EM, magnetometer and VLF-EM birds during flight via a safety shear pin connected to the helicopter hook. The major power and data cables have a quick disconnect safety feature as well. Installation is by Aerodat's crews and must be certified before surveying.

The rack contains the following:

RMS Data Acquisition System/Graphic Recorders
Data Tape Recorder Unit
Video Recording Unit
Flight Path Recording Unit
Power Distribution Unit
Magnavox MX9212 GPS Receiver
Aerodat Magnetometer Console
DSCP-99 EM Console
Herz Totem 2A VLF-EM Console

6. DATA PROCESSING AND PRESENTATION

6.1 In-field Processing

The in-field processing products were generated on site some one or two days after each survey flight. Plots of the radar altimeter data showed where the helicopter was flying too high. The differentially corrected flight paths were used to determine the quality of the line spacing. Raw magnetometer and EM plots were used to assess the quality of the survey and to determine if in fill flying had to be done.

6.2 Base Map

A base map of the area was enlarged from the 1:50,000 scale topography maps published by the Canadian Department of Energy, Mines and Resources. The NTS sheets are: 105 G/6, 105 G/5, 105 G/12, 105 F/8, and 105 F/9.

6.3 Flight Path Map

The flight path record was differentially corrected using the base station GPS and was recorded in geographic coordinates using the WGS84 Spheroid. WGS 1984 latitudes and longitudes are converted to the NAD 1927 datum for Canada, which uses the Clarke 1866 spheroid with local datum shifts of $dx=-10$ m, $dy=158$ m and $dz=187$ m. The positioning data are then converted to the UTM coordinate system using a central meridian of $129^{\circ}W$.

Processing includes speed checks to identify spikes and offsets which are removed. Positions are updated every second and expressed as eastings (x) and northings (y) in metres in the UTM projection. The flight path is drawn using linear interpolation between x,y positions from the navigation system.

The manual fiducials activated by the survey operator are shown as a small circle and labeled by fiducial number. The 24 hour clock time is shown as a small square, plotted every 30 seconds. Small tick marks are plotted every 2 seconds. Larger tick marks are plotted every 10 seconds. The line numbers are given at the start and end of each survey line. Survey lines are denoted as 10XXX series of lines, while tie lines are 80XXX series lines.

The flight path map is merged with the base map by matching UTM coordinates from the base maps and the flight path record. The match is confirmed by checking the position of prominent topographic features as recorded by manual fiducial marks or as seen on the flight path video record.

6.4 Digital Elevation Model

A **Digital Elevation Model (DEM)**, sometimes termed a **Digital Topography Map**, which is a digital representation of an elevation map has been generated and plotted as a topography map. The elevations in the DEM have been calculated from the difference between the barometric altimeter and the radar altimeter along the flight path positions. The GPS elevations were used to remove the slight drift of the barometric altimeter. There are slight levelling errors in the generated topographic data, mostly noticed by a slight herringbone ripple pattern on slopes perpendicular to the flight lines. This is caused by the radar altimeter being pointed forward slightly and by the helicopter not being horizontal all of the time. In the extreme cases where the radar altimeter has pointed too far down slope (due to the helicopter's nose up maneuver when descending down steep slopes), the data has been edited out.

The DEM maps are at a scale of 1:20,000 and are plotted in a UTM coordinate system.

6.5 Electromagnetic Survey Data

The electromagnetic data are recorded digitally at a sample rate of 10 per second with a time constant of 0.1 seconds. A two stage digital filtering process rejects major sferic events and reduces system noise.

Local sferic activity can produce sharp, large amplitude events that cannot be removed by conventional frequency domain filtering procedures. Smoothing or stacking will reduce their amplitude but may leave a broader residual response that can be confused with geological phenomena. A computer algorithm, similar to surgical mutes in digital signal processing, searches out and rejects the major sferic events.

The signal to noise ratio is further enhanced by the application of a low pass digital filter. This filter has zero phase shift which prevents any lag or peak displacement from occurring, and it suppresses only variations with a wavelength less than about 0.25 seconds. This low effective time constant gives minimal profile distortion.

Following the filtering process, a base level correction is made using EM zero levels determined during high altitude calibration sequences. The correction applied is a linear function of time that ensures the corrected amplitude of the various inphase and quadrature components is zero when no conductive or permeable source is

present. The filtered and levelled data is the basis for the determination of apparent resistivity (see below).

Apparent Conductivity

The apparent conductivity is calculated by assuming a 200 metre thick conductive layer over resistive bedrock. The computer determines the conductivity that would be consistent with the recorded inphase and quadrature response amplitudes at the selected frequency. The apparent conductivity profile data is re-interpolated onto a regular grid at a 50 metres cell size using an Akima spline technique and contoured using logarithmically arranged contour intervals. The minimum contour interval depends on the selected frequency and is in units of log(ohm.m) in logarithmic intervals of 0.1, 0.5, 1.0, 5.0 etc. The colour image palette is in terms of conductivity (the inverse of resistivity) with reds denoting high conductivity and blue denoting low conductivity.

6.6 Magnetic Data

Total Magnetic Intensity

The aeromagnetic data were corrected for diurnal variations by adjustment with the recorded base station magnetic values. This is followed by fine levelling using tie line intersection information. The corrected profile data were interpolated on to a regular grid using an Akima spline technique. A 5 by 5 Hanning filter was passed over the preliminary grid. The grid provided the basis for threading the isomagnetic contours. The minimum contour interval is 5 nT with a grid cell size of 50 m.

Calculated Vertical Magnetic Gradient

The vertical magnetic gradient is calculated from the gridded total magnetic intensity data. The calculation is based on a 17 x 17 point convolution in the space domain. The results are contoured using a minimum contour interval of 0.2 nT/m. Grid cell sizes are the same as those used in processing the total field data.

Colour Shadow Map

The colour shadow map is produced by calculating and displaying the reflectance of a surface defined by the total magnetic intensity grid and the illumination angle. The reflectance of a surface is a measure of the proportion of illuminating light which will be reflected back to an observer from the surface. The reflection at each grid cell is given by the cosine of the angle between the surface normal and a specified illumination source. Changing the illumination source direction emphasizes features normal to the source direction.

The declination and inclination of the illumination source were 214° and 45° respectively.

6.8 EM Anomaly Selection and Analysis

The main purpose of EM anomaly selection is to identify possible targets. The Aerodat automated EM picking algorithm is tuned to vertical conductors. Flat lying or shallowly dipping responses are weighed less because EM responses due to gradual changes from near surface horizontal sources are assumed to be due to lateral variation in overburden thickness or conductivity.

The EM picking algorithm seeks local maximums in the coaxial responses as the coaxial response is a single peak over a vertical conductor. In addition, the width of the conductor must be such that it is due to a discrete source – a conductor, instead of being due to broad lateral variations in near surface conductivity. The depth and the conductance of the anomaly is then derived from a computer subroutine using the assumptions of steep vertical conductivity.

For flat lying targets, the EM anomalies should either be interpreted manually or from geoelectric sections. The contours of apparent resistivity may also be used to outline this type of target. However, the apparent resistivity maps use a uniform Earth as the model for the derivations of the apparent resistivities. The conductance of discrete conductors are “diluted” in this manner and little depth information is obtained.

This is the reason why the steeply dipping conductor models are still used in areas of shallowly dipping conductivity. The automated picks still provide for, admittedly somewhat less precise than one would want, an quantitative estimate of conductance and depth of conductivity. Both of which are useful in the relative sense. The EM anomalies are also listed in digital form with the coordinates in the supplied digital archive.

Characteristic EM responses to a number of simple conductor types are shown in Appendix 2.

Anomaly Selection

EM anomalies were selected using the automated EM picker and then manually screened. The manual screening involved using the offset EM profiles to determine if the anomalies realistic or were due to noise or cultural contamination of the EM signatures. The EM offset profile were also examined for broad, wide responses

which may be due to flat lying conductive features. The most conductive of these were added to EM anomalies based on the EM profile responses.

Analysis

The remaining anomalies are characterised by the conductance and depth of burial using a thin vertical sheet like source. A numerical lookup table representing the nomograms presented in Appendix 2 is used to derive the conductance and depth of burial. Note that if the conductive source is not close to being a vertical sheet like body, the quantitative estimates of this analysis will be incorrect as the wrong model Earth would have been used.

All EM anomalies are catalogued in anomaly listings in Appendix 3. The anomaly letter, survey line, location, 4,365 Hz response amplitudes and conductance and depth estimates are also presented in Appendix 3.

7. GEOLOGY

On published geological maps, the survey area is located on the west side of the Tintina Fault in the Pelly-Cassiar Platform (Mortensen and Jilson, 1985). The Pelly-Cassiar Platform is thought to be coeval, and possibly correlative with Yukon-Tanana Terrane in the Finlayson Lake district which hosts the Kudze Kayah polymetallic deposit of Cominco, and the Wolverine deposit of Westmin/Atna.

In September of 1997, Atna Resources announced significant drill results on the Wolf Property which is located in the Pelly-Cassiar Platform. The best intersection, in WF97-07, was 25.2 metres grading 6.94% Zn, 2.78% Pb, and 138.6 g/t Ag. Massive sulphide mineralisation on the Wolf Property is hosted by pyritized felsic tuffs. The felsic tuffs are part of a unit of intermediate to felsic volcanic rocks of Mississippian age which define a northwest trending belt approximately 80 kilometres long and up to 25 kilometres wide.

The Mississippian volcano-sedimentary belt is located between Cambrian to Triassic Sediments to the northeast, and Cambrian to Silurian Sediments and Volcanics to the southwest.

7.1 Project Geology and Targets

The Wolf deposit and the favourable belt of felsic volcanics and black shales which hosts the deposit are located in the southern portion of the survey area. It is assumed that the project targets would be economic mineralisation of a similar nature to the Wolf deposit. It is believed that the Wolf deposit is a Kuroko type VMS deposit.

The Kuroko deposits occur on the flanks of rhyolite domes or caldera rims near the termination of a period of bimodal back-arc basalt/rhyolite volcanism. Commonly accompanying the Kuroko-type mineralisation is a well developed stratiform, ferruginous chert exhalite composed of clastic and chemically derived components. The exhalite is a marker bed for the ore-bearing horizon. Previous studies of the area have noted that the deposits in the area are unusual for Kuroko VMS deposits

as the volcanics are alkaline and introduced into a tension-rifted black shale basin (in LeCouteur, 1997).

The Ketz River Mine occurs in-between the survey area and the Wolf Deposit. Details on the Ketz River Mine were not readily available to the report writers. It is an oxide gold mine. Secondary targets may be gold mineralisation which is similar to the Ketz River Mine.

8. INTERPRETATION

VMS deposits are amenable to direct detection by electromagnetic methods as the massive sulphides are conductive. The nearby Kudz ze Kayah deposit was easily detected by helicopter EM systems (Holroyd and Klein, 1998). The geophysical response of the Kudz ze Kayah Deposit is that of a good EM, short strike length conductor situated to the south of a band of conductive sediments. It is also magnetic.

For Kuroko VMS deposits in general, there may or may not be an associated magnetic anomaly associated with the deposit. EM and magnetic anomalies may be useful not only in direct detection of the ore, but also to find exhalite horizons or the pyritic pipe which may be followed back to the orebodies. Therefore, any reasonable conductor located by the survey should be carefully considered. However, it should be kept in mind that other sources, including graphite, and in this case, black shales, can produce an EM response which mimics the response of any VMS conductors.

One of the sought after signatures would be fairly isolated, short strike length EM anomalies which are separated from long regional conductors (see Reed, 1981, and Holroyd and Klein, 1998). Shorter strike length anomalies are sought as these are not formational types of conductors representing uniform geological events which are not localised ore forming events. The reason for searching for isolated conductors is that a hiatus after the regional event is required before the start of the volcanism associated with the ore forming event.

Reduced scale interpretation maps are included in this report for completeness. General interpretation considerations of electromagnetic, magnetic and VLF techniques are briefly presented in Appendix 2.

8.1 Geologic Interpretation

The magnetic intensity in the survey area mostly varies between 57,800 nT to 58,250 nT with some anomalous values outside of this range. The magnetic character of the area varies from active to subdued with a few linear magnetic bodies forming trends in the various regions different magnetic texture. Overall, the geophysics gives a sense of a linear belt of mixed sediments and intermediate to felsic volcanics along with discontinuous and thin basalt flows. The magnetic quiescent areas are interpreted to be due to sediments and perhaps felsic volcanics, while the more active areas have the appearance of felsic to intermediate volcanics. The linear magnetic bodies are basalts or mafic volcanics.

The apparent resistivity values varies between 10 and 2,000 ohm-metres on the 4,765 Hz coplanar data and between 2 and 1,500 ohm-metres on the 861 Hz coplanar data. The high conductance values are indicative of conductive sediments

such as black shales. They may also be due to conductive cover, but that has not been reported and does not appear likely due to the conductive areas being located on areas of different elevations and slopes. The low conductance areas are consistent with fresh, unaltered volcanics and certain sediments such as limestones or sandstones.

There does not appear to be a significant correlation to topography or drainage systems, indicating that the EM is mapping the bedrock. There is a slight correlation with elevation at the tops of the highest mountains. The resistivity highs there are for the most part associated with a unit of active magnetic highs.

Given the abundance of long regional conductors in the survey area, the VLF shows more or less the same general trends and structure as the apparent resistivity values. The moderate to higher resistivities of the higher parts of the project area has moderated the normally strong correlation between the VLF signature and topography. Topographic highs are still seen as VLF total field maximums, but not to the degree as seen elsewhere in the world.

Based primarily on the magnetic character and on the apparent resistivity values, the area has been divided into nine distinct areas of different geophysical responses and which are interpreted to be due to different geologic units.

The first, outlined as **Sediments 1?** is located in the southeast portion of the survey area. It is separated from the other units by a marker unit which is conductive. This marker conductive unit is very continuous and shows a dip to the southwest. The unit is characterised by high apparent resistivities and a quiet magnetic character.

A second unit of sediments, labelled **Sediments 2?** is located in the north west portion of the survey area. It is in an area of TMI low, and is separated from the rest of the units by another conductive marker horizon which also correlates with a magnetic contact. The unit is characterised by low magnetic intensities, and is conductive, perhaps indicating that portions of the unit are mudstones.

The other interpreted sedimentary unit is labelled **Sediments 3?** Located in the southwest portion of the survey, it is distinguished by a semi-circular conductive and magnetic feature which apparently separates this unit from the rest. The unit is interpreted to be due to sediments as it is relatively non-magnetic and resistive. There may be some volcanics, seen as magnetic highs, intermixed with this package.

There are three long, narrow units of intermixed volcanics and sediments which have been interpreted from the geophysics based on the linear nature of the magnetic texture and the linear nature of the conductors within these units.

The first is a package of labelled as **Intermixed Intermediate to Mafic Volcanics and Conductive Sediments?** This unit is located on the northeast side of the survey. It has high magnetic values which is interpreted to be due to the intermediate to mafic volcanics. The abundance of EM conductors and the high conductance of the unit is explained by the conductive sediments (probably black shales) intermixed with the unit. In this package, there is a lack of areas of interest in the interpretation map as it is difficult to distinguish a possible sulphide source from the responses of the black shales.

At the north end of the above package is an area of relatively high magnetic values and lower conductance. It has EM conductors intermixed in the unit, but is not nearly as conductive as the Intermixed Intermediate to Mafic Volcanics and Conductive Sediments? unit. This area has been distinguished as a unit of **Intermediate Volcanics?**

To the west of the first intermixed package is an unit of **Intermixed Felsic to Intermediate Volcanics and Sediments?** Compared to the first intermixed unit, it is characterised by average (for this survey) magnetic intensities and fewer EM conductors. Notice that this unit probably hosts the known Wolf Deposit, although this was not confirmed to the report writer. As such, any EM conductor located in this unit should be examined in further detail at some time in the exploration process.

To the southwest of the survey area, is the third intermixed unit. It has the lowest magnetic values of the three intermixed units. Hence the felsic volcanic interpretation. It is interpreted to be due to a unit of **Intermixed Felsic Volcanics and Sediments?** This unit appears to be on the other side of a marker unit of magnetic highs which separates this unit from the central intermixed volcanic and sediment unit. For this reason, conductors located in this unit may be less favourable than conductors located in the Intermixed Felsic to Intermediate Volcanics and Sediments? unit.

There are two magnetic units which are clearly seen in the data. They are characterised by high magnetic and resistive values. It is possible that these magnetic units can be subdivided with more effort, but the evidence for subdivision based on geophysics is not conclusive.

The first, is a unit of **Mafic Volcanics?** This unit has very high magnetic values and is resistive. In the north and northeast of the survey area, this unit appears to be flat lying and occurs at higher elevations, as if it was a discordant cap on the general stratigraphy. Further south, it has a more linear nature and has more of a steep dip to the southwest perhaps indicating that it is a unit of basalts. To the extreme south of the survey, this unit may be an important marker unit which helps to separate the favourable stratigraphy from less favourable one.

Located in the middle portion of the survey area, and on strike with the Mafic Volcanics? is a unit interpreted to be due to **Intermediate to Mafic Volcanics?** It is less magnetic than the Mafic Volcanics? and also has a flat lying sort of response which varies in thickness. The thickest portions are outlined in the interpretation map. The unit is a magnetic high and resistivity high. Unlike the Mafic Volcanics? which is totally devoid of EM anomalies, several conductors can be seen with this unit. These EM conductors in the Intermediate to Mafic Volcanics? unit may be due to clay and water filled faults as they have a very linear nature to them.

Several magnetic lineaments are also detected and marked on the interpretation map. In general, the lineaments are detected as disruptions in the linear character of the magnetic and electromagnetic responses. These lineaments may be faults, and or fault contacts.

8.2 Electromagnetic Interpretation

The electromagnetic data are presented in terms of levelled profiles of the inphase and quadrature for the low coaxial and coplanar, and medium coaxial and coplanar frequencies and the high coplanar frequency.

There are numerous conductors located by the survey. In the EM interpretation, the conductors or zones of conductivity were interpreted from the profiles of the mid-frequency data first. The low frequency data were then interpreted to determine if a more conductive portion inside areas of widespread conductivity can be identified.

In this survey, the EM anomalies which are interpreted on a profile by profile basis show the grain and texture of the interpreted units. For this reason, select individual EM responses have been connected to emphasize this grain, or general trend of the geology. Such EM anomalies may be due to bedding planes, or to more linear units due to sediments.

In addition, a number of EM anomalies which may be indicative of mineralisation have been outlined and are described below.

8.3 Areas of interest

From an examination of the geophysical anomalies, and the interpreted geology, anomalous areas which warrant various levels of additional examination have been identified. These are all EM responses which are located in the favourable stratigraphy, have shorter strike lengths, with or without magnetic association, or exhibit complexity indicative of localised structural controls on mineralisation. Forty-six such features are located and are labelled on the interpretation map. The anomalous areas are roughly classified into three priorities or rankings with top priority being a rank of 1.

Anomaly #1 may be the Wolf Deposit as it is a fairly isolated anomaly located in the approximate area. This anomaly is longish and has better conductivity in the middle. It sits 400 to 500 metres off a conductive trend and has a dip to the northeast. There is some indication that there are closely spaced multiple conductors in the EM response. This is a top ranked anomaly due to its conductance and relative isolation from other anomalies.

Anomalies #2 is on strike with #1 and is some 600 metres to the southeast of #1. Anomaly #2 is less conductive and is of shorter strike length. It is a top ranked anomaly due to its association with Anomaly #1.

Anomaly #4 is longer than EM anomaly #2 and is in an en-echelon fashion to #2. Anomaly #3 may be a wider portion of #4. The two are top ranked anomalies.

Anomalies #5 and #6 are short strike length conductors. Both show signs of extension to the north and south. Anomaly #6 is less conductive than anomaly #5. Both are steeply dipping with a slight dip to the southeast. Both are top ranked anomalies based on their proximity to the Wolf Deposit.

Anomaly #7 is just off the conductive trend of the unit Intermixed Intermediate and Mafic Volcanics and Conductive sediments? It has good conductance values and a near vertical dip. It is also a top ranked anomaly due to its good conductance values.

Anomaly #8 is a three line EM anomaly with low conductance values. It is marked as an area of greater interest due to its proximity to Anomalies #5 and 6 and is a second ranked anomaly.

Anomaly #9A and 9B appear to be spatially related with #9A being a short EM anomaly which is steeply dipping to the southeast. Anomaly #9B is a single line anomaly. The two are second ranked anomalies.

Anomaly #10 is a low amplitude response, indicating a thin conductor or that it is farther from the EM bird (deeper, or the EM bird is higher there). It has a steep dip to the southeast. It is a second ranked anomaly due to the lower amplitudes of its response.

Anomaly #11 is a medium length EM anomaly with good conductance values. It is a local magnetic low and is trending 30 degrees across the general trend. This is a top ranked anomaly due to its conductance.

Anomalies #12 and #13 are in an en echelon fashion to #11. Anomaly #12 is a second ranked anomaly while #13 is shorter and a third ranked anomaly.

Anomaly #39 is an isolated EM anomaly with some parts having a vertical response. Its north end may be truncated by a fault and it is a third ranked anomaly.

Anomaly #40 is located in a TMI low and has short strike length. It is a third ranked anomaly.

Anomaly #41 is a three line response located in an area of average TMI values and is a third ranked anomaly.

Anomaly #42 is a complicated region of EM anomalies to the south east of the magnetic marker unit which downgrades this anomaly. This is a second ranked anomaly.

Anomaly #43 is a medium length EM response located in the same sort of magnetic setting as what is assumed to be the Wolf deposit. It has vertical dip and is flanked by shorter responses and is a top ranked anomaly.

Anomaly #44 is a more conductive area of a conductive area of ground and is on the other side of the magnetic marker horizon. It is also located in a drainage and is a third ranked anomaly.

Anomaly #45 is a shortish, good conductance response. It is located in the less favourable intermixed volcanics and sediments unit. It is a second ranked anomaly.

Anomaly #46 is parallel to #1 and is slightly less conductive. Some parts of this EM anomaly may have thickness judging from the EM profiles. It is a top ranked anomaly.

9. CONCLUSIONS AND RECOMMENDATIONS

A helicopterborne combined electromagnetic, and magnetometer survey was successfully performed over the Wolf Deposit and nearby belt in southern Yukon Territory, Canada. The geophysical data has been processed and presented at a scale of 1:20,000. The data quality exceeds or meets the contractual specifications and represents the geophysical response of the Earth.

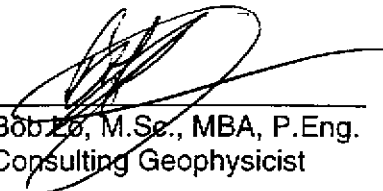
The data has then been interpreted to yield structure in terms of magnetic lineaments, and pseudo-geological units based on their geophysical responses and on known geology as supplied by Path Finder Minerals and as presented in Atna Resources' internet website.

Anomalous areas are then interpreted in terms of favourability of being due to mineralisation or indications of mineralisation. Some 46 anomalous areas have been identified which may indicate mineralisation or alteration. The top fifteen areas (areas # 1, 2, 3, 4, 5, 6, 7, 11, 19, 21, 24, 25, 38, 43, 46) should be initially prospected on the ground. The remaining areas should be correlated with known geology and geochemistry to determine if other factors such as anomalous geochemistry or favourable geologic setting will improve the rankings of the anomalies. This correlation and re-interpretation of the geophysics is of importance as many of the rankings are biased by the interpreted geological setting. There is also a lack of areas to follow up in the area of black shales as any VMS target can not be distinguished from the airborne survey alone.

The areas remaining after the initial stages of prospecting and data integration may require other geophysical methods to determine the origin of the anomaly. Ground based, geophysical methods to confirm and delineate the conductivity anomalies are recommended for those anomalies which are not found by initial prospecting. Simple magnetometer and VLF surveys may be sufficient but horizontal loop surveys are more certain to be able to detect the blind conductors.

The best of those targets after ground follow up should then be considered for drill testing.

Respectfully submitted,



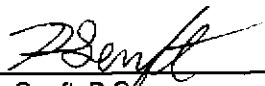
Bob Lo, M.Sc., MBA, P.Eng.
Consulting Geophysicist

for
High-Sense Geophysics Ltd.

March 3, 1998

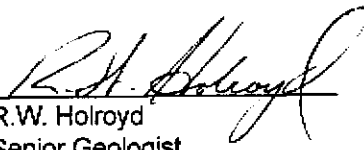
Aerodat reference: J9795

Compiled by:



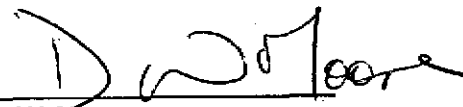
D.A. Senft, B.Sc.
Geologist I

Endorsed by:



R.W. Holroyd
Senior Geologist

Approved for
Release by:



D.W. Moore
Manager, Exploration
Western Canada

DAS/

DISTRIBUTION:
Mining Recorder (2)

REFERENCES

- Grant, F.S., and West, G.F., **Interpretation theory in applied geophysics**, McGraw-Hill Inc., Toronto, 1965.
- Gunn, P. editor, **Airborne magnetic and radiometric surveys**, AGSO Journal of Australian Geology and Geophysics, Australian Publishing Service, Canberra, 1997.
- Hood, P., *Gradient Measurements in Aeromagnetic Surveying*, **Geophysics**, vol. 30, 1965.
- Holroyd, R., Klein, J., *Geophysical Aspects of the Kudz ze Kayah Massive Sulphide Discovery, Southeastern Yukon*, in: Extended Abstracts of Pathways '98, 1998.
- Kanasewich, E.R., **Time sequence analysis in Geophysics**; University of Alberta Press, Edmonton, 1973.
- LeCouteur, P.C., *Starr Project*, a Path Finder Resources internal report, 1997.
- Mortensen, J.K., Jilson, G.A., *Evolution of the Yukon-Tanana terrane: Evidence from southeastern Yukon Territory*, **Geology**, vol. 13, 1985.
- Nabighian, M., and Macnae, J., Chapter six: Time domain electromagnetic prospecting methods, in **Electromagnetic Methods in Applied Geophysics**, Volume 2, Application, Part A, edited by M. Nabighian, Society of Exploration Geophysicist, Tulsa, 1991.
- Palacky, G.J., West, G.F., Chapter ten, Airborne Electromagnetic Methods, in **Electromagnetic Methods in Applied Geophysics**, Volume 2, Application, Part A, edited by M. Nabighian, Society of Exploration Geophysicist, Tulsa, 1991.
- Reed, L.E., *The airborne electromagnetic discovery of the Detour zinc-copper-silver deposit, Northwestern Quebec*, **Geophysics**, vol. 46, #9, 1981.

APPENDIX 1

PERSONNEL

FIELD

Flown	October 27 to November 10, 1997
Pilot	Bill Karman
Geophysical Operator (s)	Jason Cunningham
Field Geophysicist	Gregory Zimmer, B.A.Sc. Field Geophysicist

OFFICE

Processing	Andre Lambert, M.Sc., Geophysicist Liana Lambert, M.Sc., Geophysicist
Report	Bob Lo

APPENDIX 2

GENERAL INTERPRETIVE CONSIDERATIONS

Magnetometer Data

The application for magnetometer surveys is the recognition and delineation of structural or stratigraphic environments favourable for mineral deposits. Specifically, this may involve the delineation of volcanic-sedimentary contacts, intrusive bodies, faults, shears and alteration zones.

The physical parameter which the magnetic method maps is based is magnetic susceptibility and/or remanent magnetization. Generally, magnetic susceptibility is lowest in sedimentary and metasedimentary rocks. The average susceptibility of metamorphic rocks is slightly higher, being about 10 times that of sedimentary rocks. Acid igneous rocks are about twice as susceptible on average as metamorphic rocks. Ultrabasic igneous rocks have the highest susceptibilities and are about 100 times more susceptible than sedimentary rocks. The possible range of susceptibilities for any one rock type is very large and dependent upon the actual concentration of magnetic minerals, chiefly magnetite, contained within the rock.

Faults are recognised as linears and by offsets of other magnetic features. Shears and sericitic alteration zones are areas where ground water flow or alteration may have destroyed the magnetite of the host rocks. This can create areas of lower magnetic susceptibility.

The magnetometer data can be further processed in different ways. It is often filtered to produce a calculated vertical gradient map. Hood, (1965), demonstrated that in areas of steep magnetic inclination, the zero vertical gradient contour level defines the contacts of steeply dipping bodies. Vertical gradient is used to help map contacts and near surface features.

Radiometric Data

The ability to detect natural occurring radiation, whether on the ground or from an airborne platform, depends on a number of factors listed as follows:

Count Time and Detector size

Measurements or count rate statistics are more reliable the longer the detector is in position over a particular location. Therefore in airborne surveying, traverse speed is an important factor in detecting radiation sources. For this reason STOL aircraft and helicopters are a favoured platform for radiometric surveys.

The detector crystal volume and thickness determine the sensitivity of the radiometric system to radiation. For accurate measurement and differentiation of higher energy levels of radiation, a large crystal volume (minimum of 16.8 litres) is a pre-requisite.

Distance from Source (Altitude)

The attenuation or absorption of radiation in air, although not a significant factor in ground surveys, is a factor in airborne surveys. Normalization of the radiation amplitude data for altitude variations of the aircraft during the survey is necessary. The attenuation is not significant for large areal sources of radiation but is quite severe for localized point sources.

Overburden Cover

Radiation can be completely masked by one foot of rock or three feet of unconsolidated overburden.

Source Geometry

A large exposed outcrop of slightly radioactive material, such as granite which usually has a high potassium count, will be easily detectable from the air. A small outcrop of highly radioactive material, containing an appreciable amount of pitchblende for instance, may not be detectable unless the sensor passes directly over the outcrop and/or is quite close to it.

Source Characteristics

The type and percentage concentration of radioactive minerals present in the rock will determine radiation amplitudes and therefore the ability of the sensor to measure the radiation.

The above factors must be taken into consideration when evaluating and interpreting radiometric surveys. Variations in radiation amplitudes may only be a factor of overburden cover. As a result, an outcrop map of the survey area is very useful for initial evaluation of radioactive element concentrations.

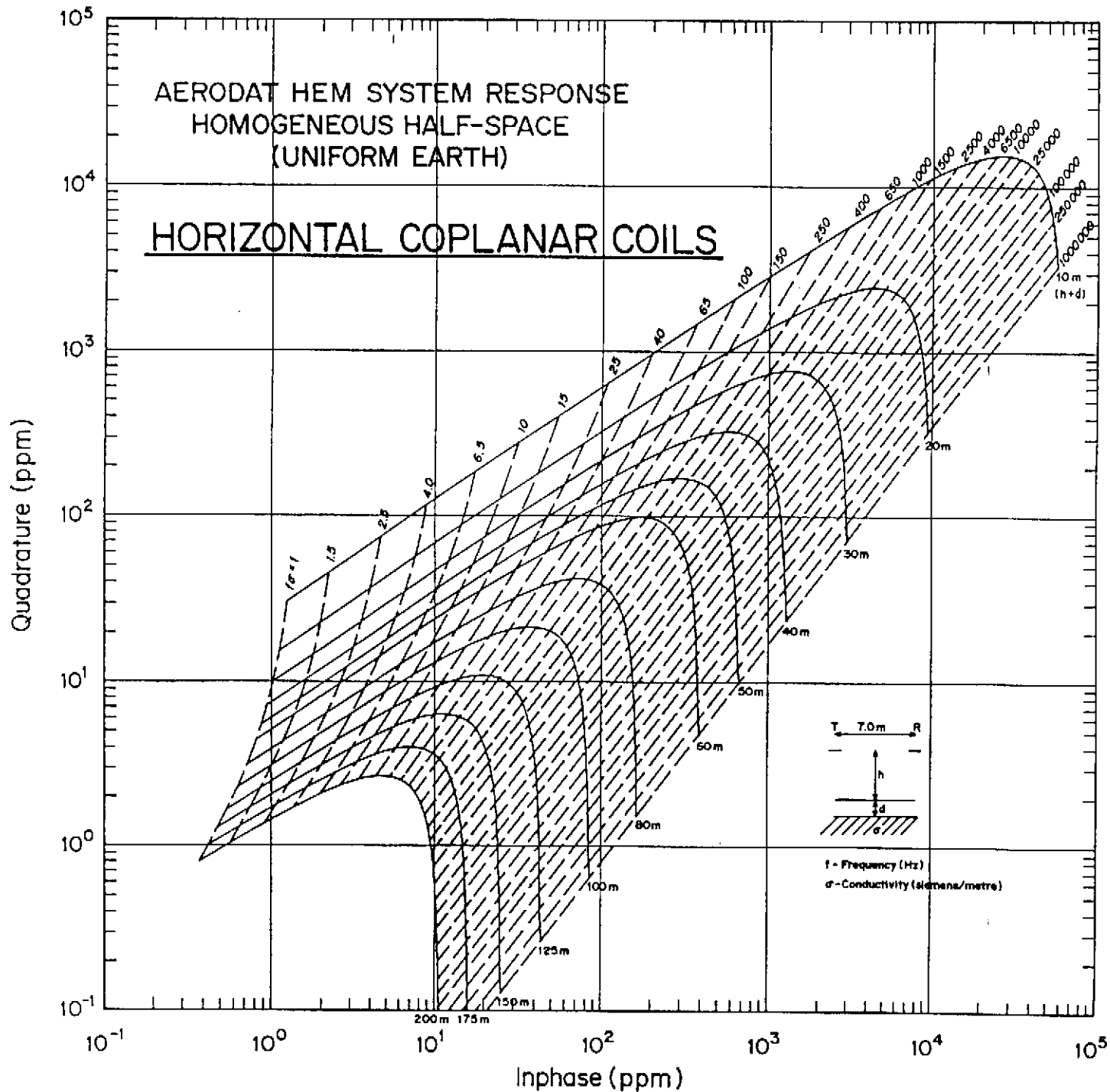
Shales and felsic intrusives tend to have high potassium and thorium levels. Mafic intrusives, sandstone and especially limestone have concentrations of one half to one tenth of the highest levels. Specific intrusives types, such as pegmatites, can have levels of potassium, uranium and thorium, in the order of three to four times the amounts normally present. Uranium ore can contain concentrations of radioactive minerals one to four orders of magnitude greater than normally encountered.

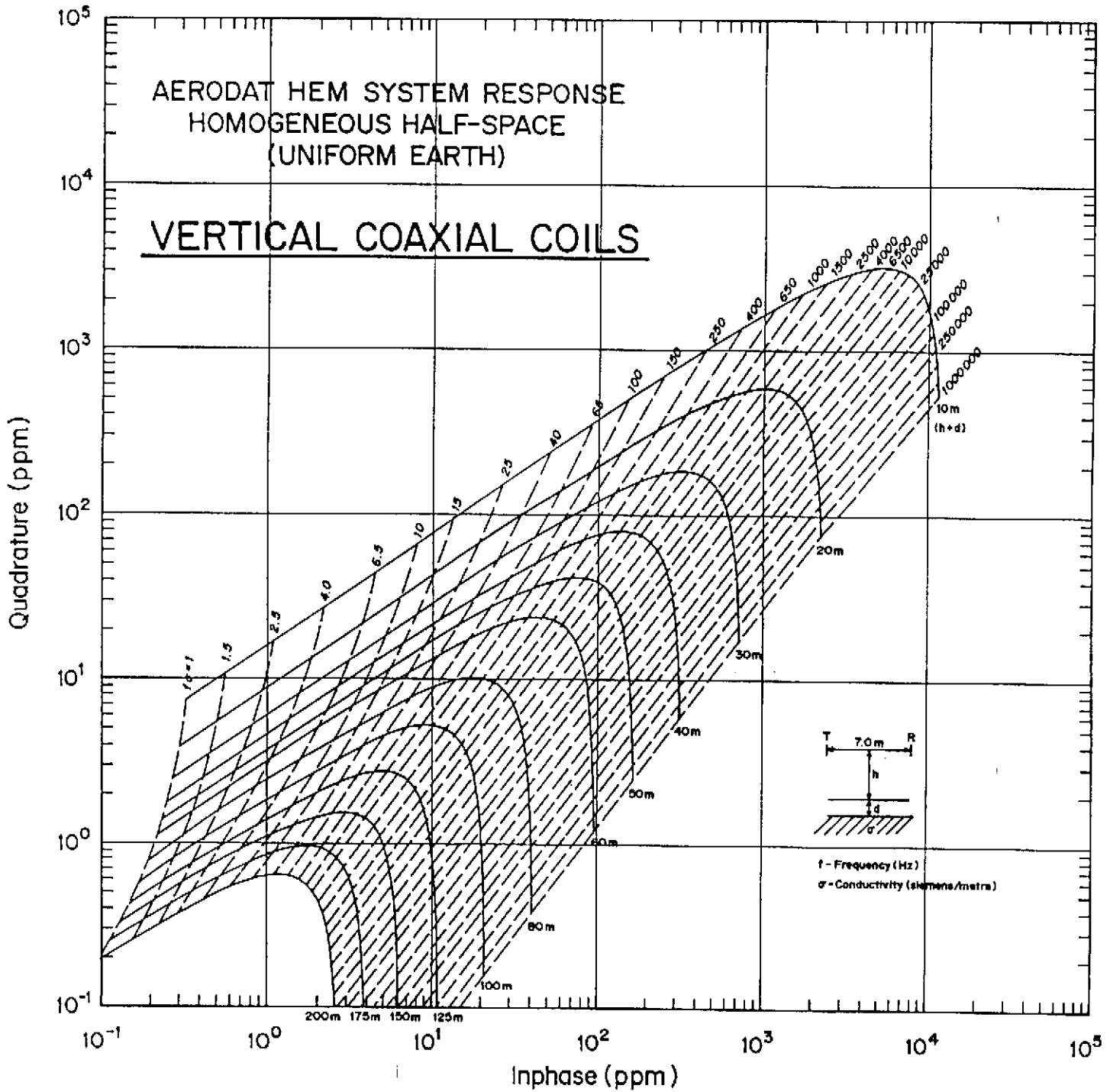
Thus, interpretation of the source of radioactive anomalies, even when the uranium, thorium and potassium thresholds are separated, can be difficult and ambiguous. In some geological environments, specific rock units have higher or lower potassium/thorium, potassium/uranium or thorium/uranium ratios. Additional diagnostic information is sometimes available when such ratio maps are generated and compared to known geological parameters.

Ideally, a transmitting station can be found which is on strike with the features of interest. This is the Line Station. The VLF station which produces a direction perpendicular to the Line Station is the Ortho Station.

Due to the relatively high frequencies of the VLF field, and to the uniform nature of the field, large regional features response well to the method. If the ground is weakly conductive, the topography influences the VLF data to a significant degree.

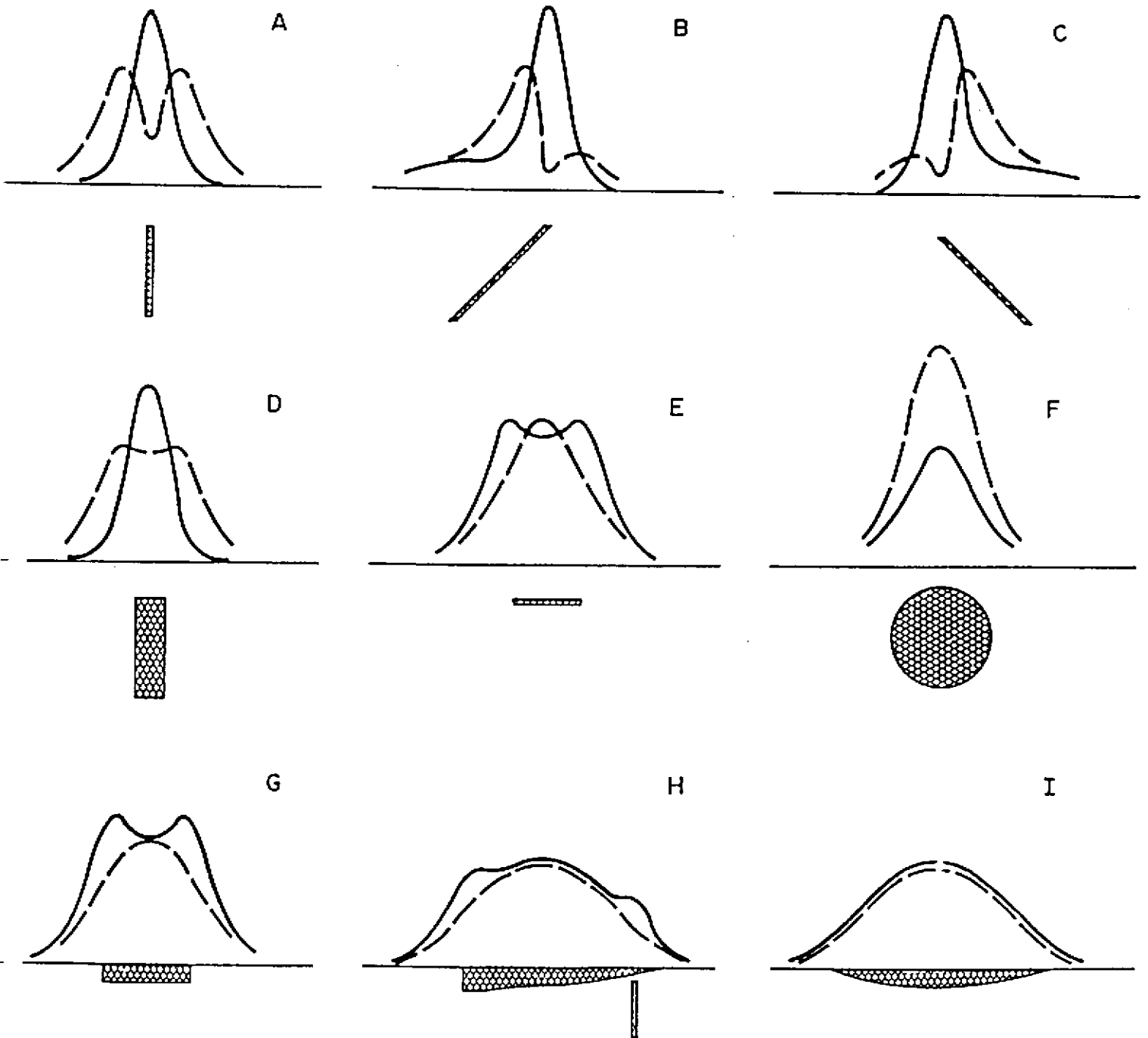
The VLF data is typically presented as contours of the total (EM) field. The VLF total field response to a steeply dipping conductor is a local maximum over the conductor.





HEM RESPONSE PROFILE SHAPE AS AN INDICATOR OF CONDUCTOR GEOMETRY

————— COAXIAL vertical scale 1 ppm/unit
 - - - - - COPLANAR vertical scale 4 ppm/unit



APPENDIX 3

ANOMALY LISTINGS

Flight	Line	Anomaly	Cat.	Inphase (ppm)	Quadrature (ppm)	Cond. (mhos)	Depth (metres)	EM bird ht. (metres)	UTM Easting (metres)	UTM Northing (metres)
21	10180	F	2	30.4	19.9	2.6	0	56	368374	6799511
21	10180	G	2	28.3	14.4	3.6	0	63	368413	6799555
21	10180	H	1	31.5	26.2	1.9	0	55	368598	6799756
21	10180	J	1	27	31.5	1.2	0	35	368968	6800194
21	10180	K	0	22.1	31.6	0.8	0	38	369009	6800268
21	10180	M	0	6.6	8.7	0.5	0	59	369086	6800398
21	10180	N	0	5.9	13.7	0.2	0	61	369550	6800814
21	10190	A	1	17.5	20.7	1	0	44	369033	6800582
21	10190	B	1	20.7	22.4	1.2	0	42	369001	6800531
21	10190	C	2	27.7	17.8	2.6	0	51	368427	6799918
21	10190	D	2	26.2	16.7	2.6	0	57	368416	6799899
21	10190	E	2	74.7	49.3	3.5	0	43	368275	6799706
21	10190	F	3	61.1	30.9	4.6	0	42	368137	6799552
21	10190	G	3	60.5	27.8	5.2	0	46	368097	6799513
21	10190	H	3	50.2	24.8	4.5	0	45	368067	6799479
21	10190	J	0	9.9	21.3	0.3	0	41	367698	6799098
21	10190	K	0	18.4	39.2	0.4	1	27	367584	6798982
21	10200	A	0	7.4	16.3	0.2	0	57	367556	6799128
21	10200	B	3	18.4	5.4	6.5	0	81	367889	6799637
21	10200	C	2	48.6	39.2	2.3	0	51	368085	6799838
21	10200	D	2	51.3	40.1	2.5	0	34	368153	6799907
21	10200	E	3	23.8	9.8	4.5	0	76	368268	6800000
22	10211	A	1	10.5	9.8	1.1	0	62	369290	6801429
22	10211	B	1	12.5	9.3	1.6	0	66	368920	6801038
22	10211	C	3	34.4	14.4	4.9	0	65	367956	6799930
22	10211	D	3	44.4	15.1	7	0	58	367831	6799842
22	10211	E	2	20.4	9.8	3.5	0	56	367731	6799733
22	10211	F	0	14.2	37.4	0.3	0	49	367241	6799176
22	10221	A	2	15.5	10	2.1	0	76	367545	6799788
22	10221	B	2	11.9	6.8	2.3	0	66	367731	6800043
22	10221	C	1	21.1	23.3	1.1	0	54	368032	6800382
22	10221	D	0	6.7	19.5	0.1	0	64	368487	6800889
22	10221	E	1	11.4	10.1	1.2	0	88	368783	6801197
22	10221	F	1	22.1	23.3	1.2	0	47	369190	6801650
22	10230	A	2	43.2	37	2.1	4	30	368649	6801357
22	10230	B	1	12.3	8	1.9	2	55	368535	6801224
22	10230	C	0	34.9	87	0.4	3	16	368421	6801096
22	10230	D	0	19.2	46.7	0.4	9	16	368409	6801084
22	10230	E	0	10.3	41.9	0.1	1	21	368393	6801069
22	10230	F	0	9.8	108.1	0	1	10	368373	6801049
22	10230	G	1	8	6.8	1.1	0	76	367936	6800561
22	10230	H	3	24.7	8.3	6	0	97	367473	6800030
22	10230	J	2	26.8	13	3.7	0	61	367373	6799912

Anomaly parameters are calculated from the response of a vertical conductive half-plane in free using the mid-frequency coaxial amplitudes.

Flight	Line	Anomaly	Cat.	Inphase (ppm)	Quadrature (ppm)	Cond. (mhos)	Depth (metres)	EM bird ht. (metres)	UTM Easting (metres)	UTM Northing (metres)
22	10240	A	3	44.3	16.1	6.4	0	86	367203	6800020
22	10240	B	3	15.2	4.9	5.4	0	89	367278	6800145
22	10240	C	2	8.5	3.9	2.7	0	70	367332	6800201
22	10240	D	0	7.5	8	0.8	0	112	368359	6801342
22	10240	E	0	44	75.1	0.8	0	44	368512	6801478
22	10250	A	1	42.1	40.1	1.8	3	29	368431	6801729
22	10250	B	1	41.1	40.1	1.7	1	31	368370	6801663
22	10250	C	1	12.3	10.5	1.3	0	59	368236	6801515
22	10250	D	0	7.5	26.2	0.1	0	39	367803	6801022
22	10250	E	1	11.4	9.6	1.3	2	52	367566	6800745
22	10250	F	3	74.1	36	5.1	0	64	367098	6800213
22	10250	G	3	152	62.1	7.9	0	36	366997	6800136
22	10250	H	3	84	40.2	5.4	0	38	366895	6800015
22	10260	A	3	206.9	111.1	6.1	0	29	366687	6800034
22	10260	B	4	166.4	61	9.3	0	37	366801	6800185
22	10260	C	2	9.9	4.7	2.8	23	43	366952	6800381
22	10260	D	1	22.9	20.3	1.6	0	60	367286	6800777
22	10260	E	2	49	31.8	3.1	0	52	367559	6801050
22	10260	F	0	20	28.9	0.8	0	62	368202	6801768
22	10260	G	1	43.1	45.5	1.6	0	55	368310	6801898
22	10260	H	0	15.9	35.6	0.4	0	41	368362	6801934
22	10270	A	3	20.2	7.5	4.9	0	56	368230	6802097
22	10270	B	1	13.5	14.6	1	1	45	368093	6801939
22	10270	C	0	8.2	8.8	0.8	9	45	368055	6801915
22	10270	D	0	9	13.1	0.5	6	39	368022	6801878
22	10270	E	1	94.6	135.9	1.4	0	27	367463	6801211
22	10270	F	3	123.9	76	4.4	0	28	367431	6801163
22	10270	G	3	73.9	34.7	5.4	0	41	367396	6801117
22	10270	H	2	26.6	20.4	2	0	53	367228	6800930
22	10270	J	2	25.1	15.2	2.7	4	41	367154	6800847
22	10270	K	1	24.2	21.1	1.6	0	62	366832	6800483
22	10270	M	4	190.3	50.9	14.5	0	56	366719	6800372
22	10270	N	4	715.1	311.2	11.3	0	25	366634	6800284
22	10270	O	3	106.1	43.2	7.2	0	29	366510	6800168
22	10270	P	3	71.4	25.1	7.7	0	42	366441	6800091
22	10280	A	3	115	53.6	6.2	0	40	366189	6800130
22	10280	B	4	130.5	42	10.3	0	31	366270	6800245
22	10280	C	4	116.2	35.8	10.6	0	37	366351	6800334
22	10280	D	3	144.1	82.7	5.1	0	36	366505	6800506
22	10280	E	0	16.9	25.1	0.7	0	41	366890	6800954
22	10280	F	0	13.3	21.4	0.5	5	31	366935	6800995
22	10280	G	2	27	17.8	2.5	0	52	367033	6801088
22	10280	H	2	62.1	39.8	3.4	0	35	367148	6801197
22	10280	J	3	90	55.6	4	0	34	367191	6801255
22	10280	K	0	14.1	18.4	0.8	0	76	367923	6802033

Anomaly parameters are calculated from the response of a vertical conductive half-plane in free using the mid-frequency coaxial amplitudes.

Flight	Line	Anomaly	Cat.	Inphase (ppm)	Quadrature (ppm)	Cond. (mhos)	Depth (metres)	EM bird ht. (metres)	UTM Easting (metres)	UTM Northing (metres)
22	10280	M	1	51.5	62.4	1.4	0	55	368078	6802226
23	10290	A	4	378	139.2	11.7	0	26	366130	6800376
23	10290	B	3	331.8	179	7	0	23	366206	6800468
23	10290	C	2	217.6	210.1	3	0	22	366285	6800557
23	10290	D	1	53.2	56.5	1.7	11	18	366367	6800640
23	10290	E	2	10.5	4.7	3	27	38	366691	6800966
23	10290	F	2	21.7	15.8	2	0	47	366775	6801055
23	10290	G	2	38	20.6	3.6	0	52	366884	6801169
23	10290	H	2	37.1	28.2	2.3	0	36	366983	6801292
23	10290	J	2	79.7	54.9	3.3	1	28	367049	6801384
23	10290	K	0	5.1	10.5	0.2	5	40	367499	6801865
23	10290	M	1	12.7	11	1.3	0	64	367714	6802094
23	10290	N	1	27.8	33.4	1.1	0	66	367755	6802160
23	10290	O	3	122.1	81.3	4	0	53	367931	6802328
23	10290	P	0	51.5	124.7	0.6	0	22	367983	6802390
21	10300	A	0	28.2	46.6	0.7	5	23	367598	6802207
21	10300	B	0	25.7	44.2	0.7	1	27	367557	6802177
21	10300	C	0	18.7	31.5	0.6	2	30	367523	6802146
21	10300	D	0	8.8	28.6	0.1	2	25	367477	6802094
21	10300	E	0	10.2	11.6	0.8	4	45	367278	6801864
21	10300	F	0	8.5	23.9	0.2	0	34	367176	6801748
21	10300	G	2	57.8	43.7	2.7	0	45	366956	6801499
21	10300	H	2	39.7	27.6	2.6	0	43	366865	6801381
21	10300	J	2	49.3	42.6	2.1	0	35	366674	6801209
21	10300	K	1	43.9	43.9	1.7	0	32	366595	6801117
21	10300	M	1	33.8	32.8	1.6	1	34	366534	6801042
21	10300	N	2	34.3	17.9	3.7	0	57	366138	6800602
21	10300	O	4	89.1	30.5	8.5	0	49	365963	6800425
21	10310	A	3	95	35.7	7.7	0	43	365780	6800482
21	10310	B	3	95.4	42.2	6.2	0	41	365816	6800535
21	10310	C	1	18.3	21.3	1	9	30	365937	6800704
21	10310	D	2	35.2	27	2.2	0	37	366122	6800902
21	10310	E	2	100.7	101	2.2	0	32	366388	6801182
21	10310	F	1	94.9	166.7	1.1	0	26	366458	6801266
21	10310	G	2	101.8	88.8	2.7	0	26	366571	6801385
21	10310	H	1	72.7	97.6	1.4	0	25	366657	6801480
21	10310	J	2	88.9	95.1	2	5	18	366713	6801550
21	10310	K	2	63.7	55.6	2.3	0	30	366777	6801673
21	10310	M	0	19.1	42.9	0.4	8	19	366996	6801931
21	10310	N	0	31.2	80	0.4	0	35	367400	6802389
21	10310	O	2	46.9	29.8	3.1	0	55	367616	6802611
21	10320	A	2	53.6	33.5	3.3	0	47	367539	6802795
21	10320	B	3	60.4	30.1	4.7	0	47	367502	6802745
21	10320	C	1	12.9	12.1	1.2	0	50	367287	6802511
21	10320	D	0	19.4	41.9	0.4	2	25	366904	6802080

Anomaly parameters are calculated from the response of a vertical conductive half-plane in free using the mid-frequency coaxial amplitudes.

Flight	Line	Anomaly	Cat.	Inphase (ppm)	Quadrature (ppm)	Cond. (mhos)	Depth (metres)	EM bird ht. (metres)	UTM Easting (metres)	UTM Northing (metres)
21	10320	E	2	33.1	24.9	2.2	0	41	366586	6801708
21	10320	F	1	23.9	28.1	1.1	0	45	366452	6801562
21	10320	G	1	23.1	25.9	1.1	3	34	366320	6801401
21	10320	H	1	26.2	28.3	1.3	0	40	366272	6801340
21	10320	J	1	14.9	15.9	1	3	41	366200	6801254
21	10320	K	0	12	28.8	0.3	4	26	366072	6801115
21	10320	M	0	9.3	9.5	0.9	10	43	365897	6800924
21	10320	N	3	61	31.3	4.5	0	54	365685	6800689
21	10330	A	3	53.4	23.6	5.3	0	45	365478	6800737
21	10330	B	0	21.1	26.8	0.9	6	30	366133	6801474
21	10330	C	2	52.2	43.3	2.3	0	38	366364	6801777
21	10330	D	1	41.4	46.1	1.4	5	25	366456	6801868
21	10330	E	1	51.4	52.8	1.7	1	28	366492	6801909
21	10330	F	0	18.5	27.7	0.7	0	43	366718	6802217
21	10330	G	1	11.1	9.7	1.2	0	95	367014	6802501
21	10330	H	0	10.2	17	0.5	0	77	367124	6802622
21	10330	J	0	9.4	19.1	0.3	0	46	367155	6802666
21	10330	K	2	81.3	52.7	3.6	0	51	367373	6802903
21	10330	M	1	53.6	53.9	1.8	0	39	367420	6802952
21	10340	A	2	64.7	39.8	3.6	0	36	367316	6803122
21	10340	B	1	17.9	15.6	1.5	0	50	366819	6802634
21	10340	C	0	8.8	28.6	0.1	0	32	366702	6802482
21	10340	D	1	36.1	44	1.2	3	27	366351	6802071
21	10340	E	1	17	19.7	1	0	56	366197	6801892
21	10340	F	0	13.4	28.7	0.4	0	49	365617	6801264
21	10340	G	0	12.6	19.8	0.6	0	60	365586	6801215
21	10340	H	0	15.9	26.3	0.6	0	65	365482	6801058
21	10340	J	0	12.6	22.4	0.5	0	46	365422	6800975
21	10350	A	1	31.6	30.1	1.6	0	38	365299	6801179
21	10350	B	1	36.4	43.1	1.3	0	36	365364	6801245
21	10350	C	1	38.3	40.5	1.5	4	27	365414	6801310
21	10350	D	1	13.9	11.2	1.5	0	68	365554	6801488
21	10350	E	2	29.8	21.9	2.2	0	48	365715	6801700
21	10350	F	0	13.3	20.9	0.6	33	4	365891	6801883
21	10350	G	1	28.8	30.3	1.4	0	37	366023	6801981
21	10350	H	1	22	21.1	1.4	15	25	366077	6802038
21	10350	J	1	15.7	15.4	1.2	0	88	366322	6802284
21	10350	K	0	12.9	16.8	0.7	0	60	366379	6802337
21	10350	M	0	16.5	19.8	0.9	0	72	366670	6802714
21	10350	N	1	25.3	30.2	1.1	0	54	367189	6803276
21	10360	A	2	24.2	18.3	2	0	55	367094	6803430
21	10360	B	0	11.6	20.3	0.5	0	44	366772	6803133
21	10360	C	1	16	15.8	1.2	0	65	366125	6802406
21	10360	D	1	23.7	19.6	1.7	0	75	365919	6802154
21	10360	E	1	18.3	18.6	1.2	0	59	365687	6801947

Anomaly parameters are calculated from the response of a vertical conductive half-plane in free using the mid-frequency coaxial amplitudes.

Flight	Line	Anomaly	Cat.	Inphase (ppm)	Quadrature (ppm)	Cond. (mhos)	Depth (metres)	EM bird ht. (metres)	UTM Easting (metres)	UTM Northing (metres)
21	10360	F	1	39.7	45.5	1.4	0	49	365591	6801779
21	10360	G	1	63.2	63.6	1.9	0	44	365531	6801715
21	10360	H	1	20.2	22.6	1.1	0	48	365402	6801592
21	10360	J	0	31.6	45	0.9	0	40	365232	6801376
21	10360	K	0	24.8	36.5	0.8	0	43	365178	6801301
21	10360	M	0	19.1	31	0.6	0	43	365116	6801214
21	10370	A	0	27.7	42.7	0.8	0	34	364908	6801344
21	10370	B	1	24.4	28.5	1.1	0	37	364979	6801412
21	10370	C	1	22.4	20.4	1.5	0	41	365112	6801586
21	10370	D	2	36.6	28.3	2.2	6	31	365147	6801649
21	10370	E	2	37.1	31	2	6	30	365186	6801703
21	10370	F	1	12.9	11.4	1.3	25	25	365418	6801993
21	10370	G	0	14.2	16.4	0.9	6	37	365588	6802167
21	10370	H	1	19.1	14.4	1.8	11	36	365681	6802267
21	10370	J	1	16	15.5	1.2	9	36	365855	6802413
21	10370	K	0	12.6	14.8	0.8	22	22	365928	6802480
21	10370	M	0	10.9	14.9	0.6	2	41	365976	6802540
21	10370	N	1	11.4	11	1.1	0	117	366867	6803545
21	10370	O	2	28.4	21.9	2	0	87	366906	6803623
23	10380	A	1	11.2	10.1	1.2	0	75	366385	6803383
23	10380	B	0	9.9	16.3	0.5	0	41	366118	6803081
23	10380	C	0	14.2	26.6	0.4	3	30	366011	6802961
23	10380	D	0	10.7	19	0.4	16	21	365970	6802919
23	10380	E	1	53.3	58.4	1.6	0	34	365810	6802728
23	10380	F	3	18.4	7.8	4	0	68	365488	6802343
23	10380	G	2	27	13.1	3.7	0	73	365301	6802146
23	10380	H	2	26.9	20.2	2.1	3	38	365026	6801850
23	10380	J	2	45	32.1	2.7	0	50	364950	6801775
23	10380	K	0	20.9	27.8	0.9	0	56	364833	6801644
23	10390	A	1	34.1	41	1.2	0	38	364722	6801782
23	10390	B	1	45.2	52.8	1.4	0	33	364780	6801858
23	10390	C	1	32.3	30.7	1.6	8	27	364855	6801965
23	10390	D	1	26.9	29.8	1.2	6	29	365074	6802154
23	10390	E	2	35.9	26.5	2.4	0	49	365153	6802216
23	10390	F	2	89.4	65.1	3.2	0	32	365216	6802267
23	10390	G	3	54.1	25.3	4.9	0	44	365334	6802429
23	10390	H	2	57.8	35	3.6	0	41	365364	6802456
23	10390	J	2	36.6	24.7	2.7	13	25	365453	6802568
23	10390	K	1	38.7	39.1	1.6	0	43	365607	6802765
23	10390	M	2	24.9	16.2	2.5	0	60	365635	6802819
23	10390	N	0	24	79.3	0.2	6	13	365759	6802981
23	10390	O	0	17.2	114	0.1	0	28	365813	6803024
23	10390	P	0	8.3	8.3	0.9	0	85	366067	6803251
23	10390	Q	0	8.6	10.5	0.7	0	67	366207	6803455
23	10390	R	0	19.9	24.6	0.9	0	47	366259	6803522
23	10390	S	3	154.8	77.1	6.2	0	43	366525	6803771

Anomaly parameters are calculated from the response of a vertical conductive half-plane in free using the mid-frequency coaxial amplitudes.

Flight	Line	Anomaly	Cat.	Inphase (ppm)	Quadrature (ppm)	Cond. (mhos)	Depth (metres)	EM bird ht. (metres)	UTM Easting (metres)	UTM Northing (metres)
23	10390	T	3	165.6	76.8	6.9	0	48	366549	6803795
23	10400	A	3	226.3	113.7	6.8	1	20	366321	6803881
23	10400	B	2	257.6	300.3	2.5	0	17	366134	6803638
23	10400	C	1	150.3	234.9	1.5	0	18	366108	6803609
23	10400	D	2	30.1	20.5	2.5	5	36	365839	6803338
23	10400	E	0	9.6	30.9	0.1	7	20	365661	6803134
23	10400	F	0	24.8	61.9	0.4	3	19	365611	6803057
23	10400	G	1	27.9	24.8	1.7	3	35	365501	6802937
23	10400	H	1	18.1	14.9	1.6	21	25	365379	6802817
23	10400	J	3	127.3	76.5	4.6	0	40	365111	6802491
23	10400	K	3	148	63.2	7.4	0	39	365088	6802471
23	10400	M	2	47.1	33.4	2.7	0	57	364965	6802328
23	10400	N	2	62.6	39.8	3.4	0	49	364916	6802259
23	10400	O	0	19.6	33.5	0.6	0	40	364714	6802037
23	10400	P	0	26.1	41.8	0.7	0	38	364648	6801951
23	10400	Q	2	68.9	56.2	2.6	0	38	364567	6801860
23	10400	R	1	17.7	19.7	1	0	41	364475	6801752
23	10410	A	1	22.4	18.1	1.8	0	44	364364	6801899
23	10410	B	1	20.3	22.5	1.1	0	50	364467	6802038
23	10410	C	1	20.1	18.6	1.4	0	59	364611	6802195
23	10410	D	2	34.6	26.2	2.2	0	44	364710	6802304
23	10410	E	2	32.3	26.1	2	0	37	364760	6802372
23	10410	F	3	58.7	30	4.5	5	30	364864	6802505
23	10410	G	2	65.1	47.2	2.9	3	27	364900	6802544
23	10410	H	1	9.7	9.5	1	0	63	365222	6802936
23	10410	J	2	57.6	48.4	2.3	0	37	365359	6803078
23	10410	K	2	53.9	36.2	3	0	39	365652	6803420
23	10410	M	1	22.7	22.6	1.3	0	48	365769	6803566
23	10410	N	3	49.4	26.3	4	0	53	365896	6803705
23	10410	O	3	57.3	25.6	5.3	0	53	365949	6803763
23	10410	P	3	77.8	29	7.3	0	50	366081	6803921
23	10420	A	3	185.6	87.5	7	0	27	365958	6804086
23	10420	B	2	95.1	96.6	2.2	0	28	365867	6803974
23	10420	C	3	290.5	149.9	7.1	0	25	365783	6803852
23	10420	D	1	27	32.2	1.1	0	38	365667	6803719
23	10420	E	2	101.6	65.7	3.9	7	20	365489	6803563
23	10420	F	0	15.6	43.3	0.3	0	25	365338	6803389
23	10420	G	0	21.6	34.1	0.7	0	35	365297	6803334
23	10420	H	2	27.5	21.6	2	0	45	365231	6803253
23	10420	J	2	38.8	24.6	3	0	44	365170	6803191
23	10420	K	2	36.3	30.3	2	0	39	365145	6803173
23	10420	M	1	25.5	24.8	1.4	16	22	365097	6803132
23	10420	N	1	9.9	9	1.1	30	24	365014	6803033
23	10420	O	2	86	64	3.1	0	43	364707	6802676
23	10420	P	2	78	64.3	2.6	0	36	364574	6802540
23	10420	Q	2	62.7	51.2	2.5	0	39	364498	6802449

Anomaly parameters are calculated from the response of a vertical conductive half-plane in free using the mid-frequency coaxial amplitudes.

Flight	Line	Anomaly	Cat.	Inphase (ppm)	Quadrature (ppm)	Cond. (mhos)	Depth (metres)	EM bird ht. (metres)	UTM Easting (metres)	UTM Northing (metres)
23	10420	R	1	40.9	36.9	1.9	0	45	364431	6802356
23	10420	S	1	42.2	51.5	1.3	0	32	364353	6802241
23	10420	T	1	40	46.7	1.3	0	44	364197	6802038
23	10430	A	1	37.4	42.6	1.3	3	27	364067	6802218
23	10430	B	1	32.3	31.6	1.6	0	48	364193	6802331
23	10430	C	2	58.1	48.8	2.3	0	31	364275	6802419
23	10430	D	2	71.6	47.7	3.4	0	31	364357	6802531
23	10430	E	2	67.2	40.7	3.7	0	40	364409	6802608
23	10430	F	2	91.4	62.3	3.5	0	29	364497	6802717
23	10430	G	2	105.8	87.6	2.9	0	25	364541	6802767
23	10430	H	1	65.1	78.4	1.5	1	23	364590	6802832
23	10430	J	2	47.8	32.4	2.9	1	34	364667	6802933
23	10430	K	2	23.6	12.7	3.1	0	54	364809	6803112
23	10430	M	2	57	52.4	2.1	0	46	365092	6803372
23	10430	N	0	14.3	38.7	0.3	0	32	365160	6803484
23	10430	O	3	126.9	79.6	4.4	0	28	365351	6803698
23	10430	P	3	375.2	231.1	6.1	0	24	365665	6804042
23	10430	Q	1	103	140.4	1.5	0	21	365708	6804089
23	10430	R	3	140.1	60.5	7.2	0	31	365829	6804214
23	10440	A	3	44	22.8	4	0	39	365756	6804339
23	10440	B	1	22.1	18.5	1.7	5	38	365643	6804215
23	10440	C	3	54.4	25.2	5	0	38	365567	6804140
23	10440	D	2	58.1	40.3	3	0	34	365514	6804102
23	10440	E	2	74.3	55.3	3	5	24	365269	6803830
23	10440	F	0	12.9	14.8	0.9	12	33	364976	6803519
23	10440	G	0	12.7	16.4	0.7	1	41	364915	6803458
23	10440	H	1	17.5	14.9	1.5	0	50	364841	6803372
23	10440	J	1	14.6	14	1.2	12	35	364685	6803209
23	10440	K	2	359	351.2	3.4	0	17	364345	6802823
23	10440	M	3	234.2	140.9	5.5	0	21	364246	6802706
23	10440	N	3	93.3	51.4	4.7	0	29	364176	6802614
23	10440	O	2	25.6	19.3	2	0	53	364063	6802474
23	10440	P	2	78.6	67.9	2.5	0	36	363962	6802348
23	10450	A	1	30.1	31.3	1.4	0	36	363608	6802292
23	10450	B	2	52.9	49.7	2	0	31	363656	6802352
23	10450	C	2	34.8	23	2.7	0	43	363809	6802564
23	10450	D	2	43.7	23.1	3.9	0	55	364051	6802828
23	10450	E	3	69.6	32.6	5.3	0	45	364179	6802953
23	10450	F	2	31.2	21.4	2.5	0	50	364308	6803098
23	10450	G	1	18.8	16.6	1.5	3	41	364384	6803180
23	10450	H	0	7.3	8.7	0.6	18	36	364516	6803323
23	10450	J	0	6.1	26.9	0.1	0	34	364960	6803860
23	10450	K	0	18.1	22.8	0.9	0	56	365142	6804052
23	10450	M	3	70.9	34.1	5.1	0	35	365348	6804260
23	10450	N	1	40	37.1	1.8	3	30	365383	6804309
23	10450	O	1	18.7	16.2	1.5	0	85	365453	6804393

Anomaly parameters are calculated from the response of a vertical conductive half-plane in free using the mid-frequency coaxial amplitudes.

Flight	Line	Anomaly	Cat.	Inphase (ppm)	Quadrature (ppm)	Cond. (mhos)	Depth (metres)	EM bird ht. (metres)	UTM Easting (metres)	UTM Northing (metres)
23	10450	P	3	76.5	37	5.2	0	68	365574	6804487
23	10450	Q	3	87.8	36.3	6.7	0	60	365591	6804509
19	10460	A	1	36.9	37.5	1.6	0	34	363403	6802407
19	10460	B	2	37.2	29.6	2.2	7	29	363603	6802622
19	10460	C	3	30.5	11.7	5.3	0	57	363833	6802835
19	10460	D	3	60.5	31.4	4.4	0	50	363918	6802938
19	10460	E	2	42.9	22.7	3.9	0	51	364008	6803047
19	10460	F	2	30.8	18.7	2.9	0	51	364169	6803219
19	10460	G	2	26.8	20	2.1	0	55	364294	6803332
19	10460	H	2	29.4	22.8	2.1	0	51	364346	6803390
19	10460	J	1	11	8.9	1.4	12	43	364432	6803509
19	10460	K	0	13	15.4	0.8	0	51	364904	6804054
19	10460	M	1	9.2	9	1	0	74	364981	6804143
19	10460	N	2	31.3	22.6	2.3	0	59	365179	6804341
19	10460	O	1	26	31.8	1.1	0	34	365235	6804411
19	10460	P	2	15	6.7	3.4	0	101	365434	6804593
19	10460	Q	0	9.4	32.2	0.1	0	29	365613	6804901
19	10470	A	3	14.3	4.8	5	6	55	365230	6804812
19	10470	B	2	48.6	42.9	2.1	0	41	364990	6804512
19	10470	C	1	24.2	21.9	1.6	0	50	364845	6804362
19	10470	D	1	18.4	22.1	1	0	46	364794	6804299
19	10470	E	1	22.7	21.6	1.4	0	58	364076	6803420
19	10470	F	2	86	71.4	2.7	0	42	363835	6803161
19	10470	G	2	107.1	92.4	2.8	0	33	363788	6803105
19	10470	H	2	106.3	74.4	3.6	0	31	363758	6803064
19	10470	J	2	40	20.9	3.9	0	54	363641	6802920
19	10470	K	1	20.8	18.7	1.5	15	27	363506	6802767
19	10470	M	1	39.7	52.4	1.1	0	37	363240	6802469
19	10470	N	3	116.2	59.9	5.4	0	43	363139	6802368
19	10480	A	0	18.4	27.2	0.7	0	43	362977	6802517
19	10480	B	1	39.5	45.1	1.4	4	26	363237	6802797
19	10480	C	0	19.9	27.2	0.8	7	28	363285	6802846
19	10480	D	2	76.8	54.6	3.2	0	47	363510	6803130
19	10480	E	2	43.4	24.4	3.6	0	44	363724	6803371
19	10480	F	2	19.3	8.6	3.8	0	57	363848	6803492
19	10480	G	0	12.7	15.4	0.8	0	48	364742	6804574
19	10480	H	0	14.8	16.8	0.9	0	62	364800	6804635
19	10480	J	4	128.5	40.3	10.6	0	57	364974	6804789
19	10480	K	4	141.2	53.3	8.6	0	42	365047	6804870
19	10480	M	0	9.5	20.5	0.3	0	40	365188	6805021
19	10490	A	1	22.6	20.7	1.5	8	33	364989	6805105
19	10490	B	3	172.7	117.9	4.3	0	25	364885	6804968
19	10490	C	0	34.1	60.2	0.7	7	18	364692	6804762
19	10490	D	0	9	10.9	0.7	11	38	363879	6803839
19	10490	E	0	8.5	15.7	0.4	0	40	363812	6803742

Anomaly parameters are calculated from the response of a vertical conductive half-plane in free using the mid-frequency coaxial amplitudes.

Flight	Line	Anomaly	Cat.	Inphase (ppm)	Quadrature (ppm)	Cond. (mhos)	Depth (metres)	EM bird ht. (metres)	UTM Easting (metres)	UTM Northing (metres)
19	10490	F	2	37.7	22.9	3.1	0	49	363711	6803613
19	10490	G	3	66.1	36.4	4.2	0	46	363625	6803527
19	10490	H	2	58.8	33.5	3.9	0	46	363575	6803471
19	10490	J	2	76.6	72	2.2	0	37	363417	6803301
19	10490	K	2	105.1	113.4	2.1	5	17	363288	6803154
19	10490	M	1	40.1	44	1.4	0	32	363219	6803058
19	10490	N	0	19.5	26.5	0.8	0	39	363077	6802924
19	10500	A	0	5.7	13.5	0.2	0	43	362779	6802885
19	10500	B	0	37.3	103.1	0.4	0	20	362920	6803047
19	10500	C	1	54.6	56.7	1.7	0	30	363064	6803204
19	10500	D	1	42.3	46.5	1.5	0	31	363104	6803250
19	10500	E	2	17.1	7.5	3.7	0	74	363454	6803657
19	10500	F	0	7.4	7.7	0.8	0	73	364350	6804627
19	10500	G	1	15.9	11.6	1.8	0	67	364456	6804810
19	10500	H	0	17.7	22.1	0.9	0	49	364539	6804905
19	10500	J	3	83	30.8	7.5	0	37	364705	6805081
19	10500	K	3	38.2	15.2	5.4	0	65	364813	6805180
19	10510	A	0	9.2	18.3	0.3	0	42	364958	6805566
19	10510	B	2	43.1	30.3	2.7	2	33	364758	6805376
19	10510	C	3	155.9	87.1	5.4	0	34	364572	6805166
19	10510	D	1	37.8	48.3	1.2	0	29	364425	6805006
19	10510	E	1	35.9	33.6	1.7	3	31	364363	6804931
19	10510	F	0	10.1	23.4	0.3	0	35	364241	6804803
19	10510	G	0	17.1	22.4	0.8	2	36	364120	6804664
19	10510	H	0	10.3	12.5	0.7	23	25	363945	6804440
19	10510	J	0	7.6	14.3	0.3	12	29	363892	6804360
19	10510	K	2	49.5	32.1	3.1	0	48	363331	6803738
19	10510	M	2	52.5	41.7	2.4	0	42	363268	6803678
19	10510	N	1	38	46	1.2	0	33	363117	6803537
19	10510	O	1	54.2	57.7	1.7	0	35	363052	6803461
19	10510	P	1	62.3	69.3	1.7	0	32	363000	6803398
19	10510	Q	2	59.7	49.5	2.4	0	34	362934	6803325
19	10520	A	0	20.5	39.1	0.5	0	30	362681	6803336
19	10520	B	2	100	105.3	2.1	0	29	362766	6803447
19	10520	C	2	63.2	50.6	2.6	0	31	362869	6803548
19	10520	D	2	37.6	26.5	2.5	0	50	363098	6803826
19	10520	E	0	11.8	19	0.5	4	35	363523	6804306
19	10520	F	2	57.4	50.4	2.2	0	33	363705	6804508
19	10520	G	0	25.7	47.8	0.6	0	33	363767	6804566
19	10520	H	0	14.1	20.7	0.6	0	39	363920	6804727
19	10520	J	2	15.3	10.3	2	0	61	364150	6804953
19	10520	K	1	14.8	10.7	1.8	0	68	364261	6805080
19	10520	M	3	38.4	16.9	4.8	0	62	364431	6805291
19	10520	N	3	41	21	4	0	58	364505	6805353
19	10520	O	3	40.8	19.7	4.3	0	55	364636	6805484

Anomaly parameters are calculated from the response of a vertical conductive half-plane in free using the mid-frequency coaxial amplitudes.

Flight	Line	Anomaly	Cat.	Inphase (ppm)	Quadrature (ppm)	Cond. (mhos)	Depth (metres)	EM bird ht. (metres)	UTM Easting (metres)	UTM Northing (metres)
19	10530	A	3	53.6	28.5	4.1	0	38	364525	6805700
19	10530	B	2	58.9	53.1	2.1	0	29	364380	6805542
19	10530	C	2	66.2	40.2	3.7	1	31	364324	6805478
19	10530	D	2	72.4	50.5	3.2	0	36	364263	6805413
19	10530	E	2	26.1	15.3	2.9	5	39	364154	6805298
19	10530	F	1	23.8	18.4	1.9	1	42	364080	6805216
19	10530	G	2	29.9	24	2	0	39	363954	6805082
19	10530	H	0	17.8	21.5	0.9	0	46	363759	6804844
19	10530	J	3	67.8	38.2	4.1	0	34	363540	6804607
19	10530	K	0	13.6	24.4	0.5	0	34	363375	6804399
19	10530	M	2	22.9	17	2	2	42	363090	6804089
19	10530	N	1	23.2	18.5	1.8	0	46	362975	6803971
19	10530	O	2	43.3	31.9	2.5	0	35	362877	6803867
19	10530	P	1	21.4	26	1	0	36	362732	6803711
19	10530	Q	2	40.1	31.3	2.3	0	36	362636	6803623
19	10530	R	1	22.7	17.2	1.9	0	46	362571	6803558
19	10530	S	0	5.8	21	0.1	0	34	362081	6802944
19	10540	A	2	19.5	11.6	2.6	0	54	362376	6803632
19	10540	B	2	34	28.4	2	0	38	362465	6803716
19	10540	C	1	25.4	31.5	1	0	35	362514	6803766
19	10540	D	2	13.9	8.4	2.2	0	58	362630	6803912
19	10540	E	0	9.5	20.2	0.3	0	47	363354	6804767
19	10540	F	0	9.7	21.4	0.3	0	37	363413	6804842
19	10540	G	0	10.9	33.3	0.2	0	30	363553	6804993
19	10540	H	0	18.9	32.2	0.6	2	29	363782	6805236
19	10540	J	2	34.3	27.1	2.1	8	29	363943	6805384
19	10540	K	1	28.7	26.6	1.6	0	38	364041	6805498
19	10540	M	2	83.2	64.3	2.9	0	38	364164	6805619
19	10540	N	2	20.8	10.2	3.4	0	76	364395	6805885
19	10550	A	3	45.2	21.1	4.6	0	50	364258	6806033
19	10550	B	3	46.3	16	6.9	0	50	364238	6805991
19	10550	C	1	115.7	177.9	1.4	5	12	364087	6805855
19	10550	D	2	222.2	178.5	3.8	8	11	364057	6805823
19	10550	E	2	74.4	62.3	2.5	0	34	363963	6805728
19	10550	F	1	27.3	33	1.1	3	30	363885	6805629
19	10550	G	2	52.3	43.6	2.3	6	25	363798	6805537
19	10550	H	0	9.5	30.3	0.2	3	24	363553	6805246
19	10550	J	0	16.9	34.9	0.4	8	21	363331	6804974
19	10550	K	0	13.6	26.3	0.4	4	28	363260	6804892
19	10550	M	1	15.4	11	1.8	0	65	362862	6804418
19	10550	N	0	13.9	17.7	0.8	0	42	362498	6804013
19	10550	O	1	37.9	54.9	1	7	20	362386	6803907
19	10550	P	1	46	44.2	1.8	0	37	362316	6803812
19	10550	Q	1	51.2	51.6	1.8	0	51	362251	6803737
19	10550	R	0	10.3	15.5	0.5	0	68	362088	6803578
19	10550	S	0	5.7	20.6	0.1	0	32	361930	6803378

Anomaly parameters are calculated from the response of a vertical conductive half-plane in free using the mid-frequency coaxial amplitudes.

Flight	Line	Anomaly	Cat.	Inphase (ppm)	Quadrature (ppm)	Cond. (mhos)	Depth (metres)	EM bird ht. (metres)	UTM Easting (metres)	UTM Northing (metres)
23	10560	A	3	124.7	60.9	6	0	33	364088	6806134
23	10560	B	3	173.1	103.4	5.1	0	23	363965	6805977
23	10560	C	3	170.3	114.3	4.4	0	26	363859	6805871
23	10560	D	2	63.8	55.9	2.3	0	30	363716	6805704
23	10560	E	0	5.6	12.2	0.2	0	43	363419	6805360
23	10560	F	0	10.5	18.7	0.4	6	32	363229	6805140
23	10560	G	0	15.9	27.8	0.5	0	40	363059	6804945
23	10560	H	1	21.5	22.3	1.2	0	45	362750	6804581
23	10560	J	1	31.4	26.8	1.9	0	42	362631	6804468
23	10560	K	2	72.9	71.2	2.1	0	30	362148	6803968
23	10560	M	1	30.8	30.5	1.5	0	50	362044	6803830
23	10560	N	1	32.3	32.1	1.5	0	55	361921	6803674
23	10560	O	0	13.6	37.5	0.2	0	26	361856	6803591
23	10570	A	1	32	33.4	1.4	0	39	361663	6803732
23	10570	B	1	30.8	26.1	1.9	0	64	361737	6803845
23	10570	C	2	35.2	26	2.3	12	26	361982	6804110
23	10570	D	2	29.8	18.5	2.8	19	23	362011	6804181
23	10570	E	1	22.4	17.4	1.9	23	21	362040	6804225
23	10570	F	0	10.4	16.9	0.5	17	23	362151	6804295
23	10570	G	0	9.2	9.8	0.8	12	40	362297	6804521
23	10570	H	0	14.2	17.4	0.8	0	42	362537	6804773
23	10570	J	1	15.6	15.7	1.1	0	51	363596	6805884
23	10570	K	2	44.4	26.6	3.3	0	54	363785	6806062
23	10570	M	2	43	28.3	2.9	0	39	363958	6806325
23	10580	A	3	56.6	21	6.7	0	48	363846	6806460
23	10580	B	1	27.6	34.9	1	0	32	363604	6806240
23	10580	C	2	37.6	21.3	3.4	0	49	363496	6806135
23	10580	D	1	28.9	34.2	1.2	0	33	363338	6805912
23	10580	E	0	21.9	31.9	0.8	2	31	363262	6805831
23	10580	F	0	9.8	17.3	0.4	6	33	363047	6805584
23	10580	G	0	10.6	13.3	0.7	0	51	362892	6805393
23	10580	H	0	9.6	10.8	0.8	14	37	362430	6804862
23	10580	J	3	23.1	9.4	4.5	0	65	361789	6804129
23	10580	K	1	59.8	67	1.6	0	34	361617	6803930
23	10580	M	1	63.2	76.5	1.5	0	27	361541	6803843
23	10590	A	1	44.3	58.5	1.2	5	22	361312	6803896
23	10590	B	1	50.1	47.7	1.9	0	35	361426	6804019
23	10590	C	1	26.5	22.3	1.8	4	35	361608	6804238
23	10590	D	0	12.3	14.2	0.9	12	33	361671	6804280
23	10590	E	1	14.7	14	1.2	15	32	361720	6804309
23	10590	F	1	10.3	8.2	1.3	20	37	361957	6804592
23	10590	G	1	10.3	7.7	1.5	8	49	361995	6804646
23	10590	H	1	21.6	20.8	1.4	0	48	363113	6805935
23	10590	J	3	70.8	39.1	4.3	0	46	363363	6806225
23	10590	K	3	105.9	60.1	4.7	0	35	363404	6806291
23	10590	M	1	22.2	17.6	1.8	0	73	363522	6806424

Anomaly parameters are calculated from the response of a vertical conductive half-plane in free using the mid-frequency coaxial amplitudes.

Flight	Line	Anomaly	Cat.	Inphase (ppm)	Quadrature (ppm)	Cond. (mhos)	Depth (metres)	EM bird ht. (metres)	UTM Easting (metres)	UTM Northing (metres)
23	10590	N	0	31.2	45.7	0.9	0	53	363589	6806467
23	10590	O	3	56	22.1	6.2	0	53	363647	6806547
23	10590	P	4	105.5	38.1	8.4	0	54	363673	6806588
19	10600	A	1	21.1	24.9	1	3	34	361149	6804009
19	10600	B	1	22.9	26.9	1.1	0	46	361206	6804108
19	10600	C	0	14	25.5	0.5	2	32	361299	6804201
19	10600	D	2	31.1	17.3	3.3	17	26	361464	6804374
19	10600	E	2	15	8.2	2.6	0	56	361589	6804504
19	10600	F	1	10.3	7	1.7	0	60	361788	6804719
19	10600	G	1	17.6	12.7	1.9	0	65	362963	6806104
19	10600	H	3	28.9	10.3	5.8	4	43	363209	6806332
19	10600	J	2	28.7	14.7	3.6	0	48	363284	6806409
19	10600	K	3	41.3	17.4	5.2	0	66	363454	6806752
19	10610	A	3	15.5	6.2	4.1	0	83	363352	6806844
19	10610	B	3	44.2	18.4	5.4	3	36	363153	6806620
19	10610	C	2	83.6	64.6	2.9	3	24	363019	6806480
19	10610	D	4	167.2	59.3	9.8	0	28	362962	6806433
19	10610	E	0	8.9	11.7	0.6	0	49	362766	6806222
19	10610	F	0	8.7	12.8	0.5	0	46	362729	6806180
19	10610	G	0	5.3	12.9	0.2	2	38	362358	6805711
19	10610	H	0	10.7	21.4	0.4	0	57	361761	6805049
19	10610	J	0	9.3	11.2	0.7	0	77	361622	6804879
19	10610	K	0	10.4	12	0.8	0	76	361539	6804804
19	10610	M	0	10.8	11.3	0.9	0	86	361461	6804734
19	10610	N	1	23.5	22.7	1.4	0	66	361333	6804604
19	10610	O	2	41.6	28.6	2.7	0	57	361269	6804549
19	10610	P	0	84.4	160.6	0.9	0	24	361069	6804306
19	10610	Q	1	82.7	118.8	1.3	0	30	361044	6804281
19	10610	R	0	55.3	93.8	0.9	0	38	360950	6804161
19	10610	S	0	6.3	22.4	0.1	0	30	360875	6804033
19	10620	A	2	23.1	15.2	2.4	0	65	360835	6804264
19	10620	B	1	30.4	40.5	1	0	40	360965	6804403
19	10620	C	2	39.4	31.5	2.2	0	53	361172	6804607
19	10620	D	0	18.6	27.5	0.7	22	12	361420	6804873
19	10620	E	1	23.9	19.4	1.8	27	15	361558	6805044
19	10620	F	1	6	4	1.4	0	102	362201	6805754
19	10620	G	0	9.5	11.9	0.7	0	77	362463	6806022
19	10620	H	0	9.5	10.5	0.8	0	62	362639	6806238
19	10620	J	3	44.7	16.4	6.4	8	32	362820	6806468
19	10620	K	1	43.7	64.1	1	0	31	362882	6806543
19	10620	M	2	36.5	26.8	2.4	9	29	362913	6806594
19	10620	N	3	22.1	7.7	5.5	0	83	362974	6806730
19	10620	O	2	22.5	11	3.5	0	89	363156	6806895
19	10620	P	3	15.8	5.4	5.1	0	97	363258	6807048
18	10630	A	2	106.1	71.3	3.8	0	33	360711	6804435

Anomaly parameters are calculated from the response of a vertical conductive half-plane in free using the mid-frequency coaxial amplitudes.

Flight	Line	Anomaly	Cat.	Inphase (ppm)	Quadrature (ppm)	Cond. (mhos)	Depth (metres)	EM bird ht. (metres)	UTM Easting (metres)	UTM Northing (metres)
18	10630	B	2	28.5	19.6	2.4	6	35	360790	6804541
18	10630	C	1	17.7	19.1	1.1	1	40	360940	6804752
18	10630	D	0	9.7	22.5	0.3	0	50	361563	6805431
18	10630	E	0	17.3	61.9	0.2	0	22	362036	6805964
18	10630	F	1	12.2	12.1	1.1	0	56	362483	6806449
18	10630	G	2	48	33.7	2.8	0	52	362715	6806741
18	10630	H	2	45.5	30.4	2.9	0	50	362771	6806814
18	10630	J	2	13.7	7.6	2.5	0	99	362961	6807012
18	10630	K	2	14.2	7.3	2.8	0	120	363100	6807221
18	10630	M	0	12.7	21.8	0.5	0	64	363151	6807287
18	10640	A	3	10.8	2.7	6.9	1	67	363039	6807366
18	10640	B	3	28.6	11.3	5	0	46	362916	6807224
18	10640	C	2	29.2	14.6	3.7	0	45	362877	6807185
18	10640	D	1	17.7	17.9	1.2	11	32	362779	6807102
18	10640	E	1	30.5	30.7	1.5	19	16	362616	6806919
18	10640	F	1	62.1	72.8	1.5	10	15	362558	6806874
18	10640	G	1	11.9	10.3	1.3	0	81	361744	6805974
18	10640	H	2	22.2	11.5	3.2	0	67	361675	6805891
18	10640	J	1	14.3	14.8	1.1	0	61	361072	6805219
18	10640	K	0	11.5	16.2	0.6	6	35	361011	6805118
18	10640	M	1	10.1	7.6	1.4	15	43	360921	6805059
18	10640	N	0	18.3	24.8	0.8	0	62	360779	6804891
18	10640	O	2	47	26	3.8	0	57	360506	6804567
18	10640	P	2	36.7	23.8	2.8	0	51	360438	6804481
18	10650	A	3	47.5	24.4	4.2	0	52	360376	6804722
18	10650	B	2	25.1	13.3	3.2	0	54	360436	6804832
18	10650	C	1	32.7	45.7	1	5	24	360627	6805017
18	10650	D	1	34.6	31.7	1.7	4	31	360724	6805142
18	10650	E	2	48.4	43.9	2	5	26	360798	6805231
18	10650	F	1	46.8	48.6	1.6	11	18	360907	6805357
18	10650	G	0	23.8	31	0.9	24	10	360975	6805454
18	10650	H	0	17.7	37.2	0.4	0	37	361041	6805528
18	10650	J	0	14.3	37.1	0.3	0	34	361133	6805583
18	10650	K	2	17.1	8.8	3	14	39	361423	6805969
18	10650	M	2	25	14.2	3	11	35	361535	6806095
18	10650	N	2	29.4	23.4	2	0	50	362323	6806958
18	10650	O	2	22.6	12.8	2.9	0	74	362461	6807051
18	10650	P	2	37.7	21.1	3.4	0	54	362698	6807349
18	10650	Q	2	41.9	33	2.3	0	43	362740	6807390
18	10660	A	2	40.5	28.2	2.6	0	48	362453	6807323
18	10660	B	1	13.9	13.1	1.2	14	33	362327	6807177
18	10660	C	3	41.6	21.4	4	1	38	362217	6807070
18	10660	D	2	49.6	44.7	2	2	29	361420	6806194
18	10660	E	2	28.9	18.1	2.7	1	41	361358	6806148
18	10660	F	1	9.9	7	1.6	0	68	361277	6806062
18	10660	G	0	11.4	12.1	0.9	0	49	360832	6805484

Anomaly parameters are calculated from the response of a vertical conductive half-plane in free using the mid-frequency coaxial amplitudes.

Flight	Line	Anomaly	Cat.	Inphase (ppm)	Quadrature (ppm)	Cond. (mhos)	Depth (metres)	EM bird ht. (metres)	UTM Easting (metres)	UTM Northing (metres)
18	10660	H	1	9.8	7	1.5	0	72	360533	6805232
18	10660	J	0	16.6	25.2	0.7	0	52	360422	6805079
18	10660	K	2	58.3	47.6	2.4	0	40	360285	6804967
18	10660	M	3	67.2	35.7	4.4	0	47	360167	6804839
18	10660	N	2	53.6	40.2	2.6	0	37	360082	6804736
18	10670	A	3	32.3	13.6	4.8	0	55	360046	6804922
18	10670	B	3	29	12.6	4.4	0	65	360089	6804961
18	10670	C	2	23.2	12.4	3.1	0	58	360178	6805048
18	10670	D	1	17.8	14.9	1.5	3	43	360299	6805209
18	10670	E	0	13.9	35.6	0.3	9	18	360724	6805726
18	10670	F	1	13.3	9	1.9	22	32	361185	6806265
18	10670	G	0	17.2	24	0.7	19	17	361264	6806351
18	10670	H	0	6.7	10.9	0.4	0	59	361799	6806945
18	10670	J	0	9.4	10.4	0.8	0	55	361894	6807037
18	10670	K	2	26	15.4	2.8	0	58	362031	6807184
18	10670	M	2	47.5	27.3	3.6	0	43	362126	6807326
18	10670	N	2	37.2	22.8	3	0	57	362209	6807446
18	10670	O	3	35.5	16.9	4.2	0	62	362290	6807534
18	10670	P	3	24	7.8	6.2	0	69	362388	6807625
18	10670	Q	3	25.9	11.4	4.2	0	67	362460	6807706
18	10680	A	3	85.5	34.8	6.7	0	43	362167	6807672
18	10680	B	3	125.3	82.6	4.1	0	31	361993	6807439
18	10680	C	2	74.8	51.3	3.3	6	23	361937	6807370
18	10680	D	3	109.7	53.3	5.8	0	35	361827	6807272
18	10680	E	0	10.8	13.9	0.7	6	39	361707	6807152
18	10680	F	0	11.3	15.5	0.6	10	33	361654	6807075
18	10680	G	0	7.7	9.4	0.6	0	55	361042	6806382
18	10680	H	0	20.9	28.3	0.8	0	43	360632	6805894
18	10680	J	0	14.6	18.4	0.8	0	67	360200	6805403
18	10680	K	2	38.5	32	2.1	0	58	360068	6805215
18	10680	M	2	56.8	35.3	3.4	0	53	360007	6805154
18	10680	N	2	61.2	37	3.6	0	47	359936	6805092
18	10680	O	3	56.3	27.7	4.6	0	47	359859	6805019
18	10690	A	2	43.3	23.4	3.8	0	58	359673	6805140
18	10690	B	2	51.8	29.3	3.8	0	50	359725	6805209
18	10690	C	2	55.6	36	3.2	0	42	359877	6805363
18	10690	D	2	40.5	28.7	2.6	0	38	359918	6805408
18	10690	E	0	20.6	28.6	0.8	8	27	360121	6805683
18	10690	F	2	21.5	15.6	2	0	55	360436	6806026
18	10690	G	0	6.8	6.4	0.9	0	73	360656	6806269
18	10690	H	0	5.4	11.6	0.2	0	45	361052	6806727
18	10690	J	0	6.1	13.3	0.2	0	48	361127	6806797
18	10690	K	0	10.9	26.4	0.3	2	29	361419	6807156
18	10690	M	3	57.4	20.8	7	0	37	361599	6807365
18	10690	N	3	28.3	13.1	4	0	50	361677	6807451
18	10690	O	3	43.3	20.7	4.4	0	50	361750	6807519

Anomaly parameters are calculated from the response of a vertical conductive half-plane in free using the mid-frequency coaxial amplitudes.

Flight	Line	Anomaly	Cat.	Inphase (ppm)	Quadrature (ppm)	Cond. (mhos)	Depth (metres)	EM bird ht. (metres)	UTM Easting (metres)	UTM Northing (metres)
18	10690	P	2	44.9	25.6	3.6	0	52	361795	6807560
18	10690	Q	2	63.5	39	3.6	0	59	361862	6807634
18	10690	R	3	71.1	40.5	4.1	0	57	361902	6807687
18	10690	S	2	37.7	20.7	3.5	0	47	361983	6807789
18	10690	T	4	59.9	16.8	9.9	0	55	362160	6807992
18	10700	A	3	90.9	41.1	6	0	39	362101	6808136
18	10700	B	4	130.4	50.1	8.2	0	31	362067	6808085
18	10700	C	1	56.4	60.3	1.7	0	28	361884	6807887
18	10700	D	2	259.8	355.9	2.1	0	14	361773	6807763
18	10700	E	2	230.4	317.5	2	3	11	361732	6807717
18	10700	F	3	183.5	95	6.2	3	20	361640	6807622
18	10700	G	2	33.2	19.5	3.1	12	29	361567	6807550
18	10700	H	3	29.9	9.4	6.9	1	46	361470	6807466
18	10700	J	0	10	10.8	0.9	0	57	361381	6807373
18	10700	K	1	11.4	11.9	1	1	48	361272	6807207
18	10700	M	0	11.9	23	0.4	0	58	360504	6806362
18	10700	N	1	19.2	16.7	1.5	0	64	360274	6806110
18	10700	O	1	51.1	64.5	1.3	0	32	360000	6805780
18	10700	P	2	35.1	17.6	3.9	0	65	359761	6805513
18	10700	Q	2	46	25.3	3.8	0	60	359704	6805444
18	10700	R	2	49.9	32.2	3.1	0	53	359652	6805383
18	10700	S	2	28.3	19.9	2.3	0	52	359540	6805247
18	10710	A	2	44.8	27.2	3.3	0	47	359439	6805470
18	10710	B	3	43.4	22.6	4	0	49	359502	6805529
18	10710	C	2	32.9	19.5	3.1	0	54	359613	6805624
18	10710	D	2	40.5	31.2	2.3	0	37	359811	6805846
18	10710	E	1	21.1	23.4	1.1	3	35	359877	6805941
18	10710	F	1	20	17	1.6	15	28	360008	6806051
18	10710	G	1	9.7	9.6	1	0	86	361113	6807287
18	10710	H	0	9.4	11.6	0.7	0	75	361199	6807425
18	10710	J	3	70.8	29.6	6.1	0	52	361352	6807598
18	10710	K	2	64.8	38.3	3.8	0	40	361446	6807680
18	10710	M	2	86.9	61.5	3.3	0	36	361501	6807739
18	10710	N	2	63.1	46.8	2.8	0	40	361562	6807812
18	10710	O	3	49.9	26.7	4	0	47	361608	6807871
18	10710	P	3	55.2	23.6	5.5	0	47	361835	6808168
18	10720	A	3	49.8	17.9	6.7	0	50	361796	6808396
18	10720	B	3	47.6	18.1	6.2	0	40	361678	6808216
18	10720	C	3	35.4	16	4.5	0	59	361346	6807863
18	10720	D	3	33.4	11.8	6.1	0	50	361271	6807770
18	10720	E	3	26.9	10.1	5.3	0	55	361230	6807724
18	10720	F	0	17	37	0.4	0	46	359994	6806380
18	10720	G	1	32.1	35.1	1.3	0	45	359803	6806199
18	10720	H	1	31.4	34.2	1.3	0	44	359763	6806157
18	10720	J	1	23.2	26.3	1.1	0	42	359668	6806041
18	10720	K	1	27.9	25.3	1.6	0	45	359602	6805933

Anomaly parameters are calculated from the response of a vertical conductive half-plane in free using the mid-frequency coaxial amplitudes.

Flight	Line	Anomaly	Cat.	Inphase (ppm)	Quadrature (ppm)	Cond. (mhos)	Depth (metres)	EM bird ht. (metres)	UTM Easting (metres)	UTM Northing (metres)
18	10720	M	1	17.9	15.8	1.4	0	53	359525	6805808
18	10720	N	2	33.9	22.6	2.6	0	63	359400	6805655
18	10720	O	2	33.9	23.3	2.5	0	57	359333	6805592
18	10720	P	1	19.4	15.6	1.7	0	55	359261	6805534
18	10730	A	2	32.5	16.6	3.7	0	58	359089	6805659
18	10730	B	2	38.8	23.4	3.2	0	54	359142	6805760
18	10730	C	2	29.8	20.4	2.4	0	46	359195	6805848
18	10730	D	1	19.4	14.7	1.8	0	58	359378	6806040
18	10730	E	1	15.7	11.9	1.7	0	61	359517	6806137
18	10730	F magnetite	0	-22.6	3	0	0	11	360496	6807233
18	10730	G	2	39.6	27.2	2.7	12	25	361014	6807831
18	10730	H	3	43.9	20.2	4.7	0	42	361093	6807911
18	10730	J	2	53.6	45.4	2.2	0	46	361185	6808045
18	10730	K	2	58.6	42.7	2.8	0	41	361215	6808097
18	10730	M	2	36.9	27.9	2.3	0	50	361273	6808200
18	10730	N	1	11.5	9.2	1.4	0	76	361384	6808299
18	10730	O	3	180.6	129.1	4.1	0	39	361602	6808540
18	10730	P	2	137.4	133.6	2.6	0	33	361628	6808573
17	10740	A	2	32.9	17.8	3.5	0	62	358914	6805777
17	10740	B	2	67.5	50.8	2.8	0	38	359026	6805898
17	10740	C	2	74.6	64.9	2.4	0	33	359082	6805958
17	10740	D	1	40.6	40.1	1.7	8	24	359273	6806175
17	10740	E	1	20.1	17.2	1.6	0	44	359478	6806364
17	10740	F	2	24.1	14.8	2.6	7	38	359590	6806501
17	10740	G	2	24.1	14.8	2.6	7	38	359590	6806501
17	10740	H	1	16.4	15.6	1.3	0	54	359674	6806628
17	10740	J	1	12.4	12.1	1.1	0	59	359857	6806851
17	10740	K	2	15.4	9.8	2.1	0	55	359952	6806952
17	10740	M	1	14.4	11.2	1.6	0	54	360032	6807052
17	10740	N magnetite	0	-29.2	9.1	0	0	11	360207	6807251
17	10740	O	2	21.2	13.3	2.4	0	49	360829	6807964
17	10740	P	3	28.5	12.8	4.2	0	56	360885	6808032
17	10740	Q	1	30	40.8	1	0	32	361032	6808186
17	10740	R	1	43.1	56.6	1.2	0	30	361065	6808226
17	10740	S	0	44.5	71.6	0.9	0	30	361110	6808272
17	10740	T	0	18.4	26.5	0.7	0	46	361163	6808314
17	10740	U	1	12.4	10.6	1.3	0	77	361227	6808370
17	10740	V	2	14.1	6.6	3.2	0	98	361373	6808529
17	10740	W	2	20.5	10.6	3.1	0	79	361515	6808691
17	10750	A	3	31	10.5	6.3	0	53	361260	6808715
17	10750	B	1	39.7	40.7	1.6	0	36	361154	6808589
17	10750	C	1	125.8	241.1	1.1	0	18	360999	6808351
17	10750	D	1	97.9	113.2	1.8	0	26	360970	6808304
17	10750	E	2	33.8	23.1	2.6	0	46	360873	6808220
17	10750	F	2	36.4	24.1	2.7	6	32	360802	6808142
17	10750	G	2	37	19.4	3.7	8	33	360763	6808111

Anomaly parameters are calculated from the response of a vertical conductive half-plane in free using the mid-frequency coaxial amplitudes.

Flight	Line	Anomaly	Cat.	Inphase (ppm)	Quadrature (ppm)	Cond. (mhos)	Depth (metres)	EM bird ht. (metres)	UTM Easting (metres)	UTM Northing (metres)
17	10750	H	3	45.1	19.9	5	0	44	360706	6808057
17	10750	J	2	29.3	19.6	2.5	2	39	360669	6808022
17	10750	K	3	19.2	7.5	4.5	1	53	360549	6807896
17	10750	M	1	18.1	19.8	1.1	0	49	359878	6807143
17	10750	N	1	29.3	31.6	1.3	0	53	359851	6807106
17	10750	O	1	30.8	30.2	1.5	0	55	359826	6807071
17	10750	P	1	18.3	21.1	1	0	42	359446	6806654
17	10750	Q	1	28.3	27.1	1.5	0	49	359263	6806467
17	10750	R	1	32	28.7	1.7	0	49	359201	6806395
17	10750	S	2	43.8	35.1	2.3	0	54	358936	6806120
17	10750	T	2	60.4	44	2.8	0	46	358869	6806049
17	10750	U	2	48.8	30.5	3.2	0	46	358793	6805969
17	10750	V	2	48.8	30.5	3.2	0	46	358793	6805969
17	10760	A	2	28.8	18.4	2.6	0	52	358683	6806071
17	10760	B	2	16.8	10.3	2.3	0	61	358745	6806140
17	10760	C	2	23	13.7	2.7	0	47	358986	6806456
17	10760	D	2	23	13.7	2.7	0	47	358986	6806456
17	10760	E	1	23.5	24.7	1.3	0	40	359074	6806554
17	10760	F	2	17.9	12.5	2	9	39	359142	6806643
17	10760	G	0	9.2	9.4	0.9	0	60	359304	6806796
17	10760	H	1	17.3	20.2	1	0	41	359660	6807180
17	10760	J	0	9.3	10.7	0.8	2	48	359779	6807306
17	10760	K	0	4.3	8.9	0.2	24	23	360189	6807803
17	10760	M	1	17.2	14	1.6	0	62	360304	6807936
17	10760	N	2	19.4	10.3	3	0	62	360348	6807984
17	10760	O	4	38.6	10.2	9.4	0	48	360453	6808065
17	10760	P	1	35.2	32.2	1.8	0	48	360711	6808411
17	10760	Q	0	19.6	38	0.5	8	21	360820	6808495
17	10760	R	1	19.8	23.3	1	0	56	360943	6808619
17	10760	S	3	91	44	5.5	0	40	361157	6808900
17	10770	A	4	136.7	37.1	13	0	31	361006	6808975
17	10770	B	1	8.1	5.3	1.6	34	31	360796	6808773
17	10770	C	1	114.8	156.5	1.6	13	6	360753	6808657
17	10770	D	1	106	130.9	1.7	13	7	360737	6808635
17	10770	E	2	122.4	109	2.8	5	18	360612	6808493
17	10770	F	2	28.4	13.9	3.8	2	43	360416	6808315
17	10770	G	3	32.2	10.4	6.8	0	53	360343	6808213
17	10770	H	2	23.1	12.1	3.2	5	43	360235	6808112
17	10770	J	0	9.4	16.4	0.4	0	51	359776	6807618
17	10770	K	0	9.4	16.4	0.4	0	51	359776	6807618
17	10770	M	0	10.3	19.3	0.4	0	50	359614	6807436
17	10770	N	0	11.4	21.6	0.4	0	46	359559	6807388
17	10770	O	0	8.7	21.6	0.2	0	38	359312	6807114
17	10770	P	0	13.6	18.9	0.7	0	57	359181	6806947
17	10770	Q	1	20.2	23.9	1	0	53	359094	6806864
17	10770	R	3	55.7	30.7	4	0	48	358944	6806724
17	10770	S	1	19.2	14.6	1.8	0	68	358745	6806515

Anomaly parameters are calculated from the response of a vertical conductive half-plane in free using the mid-frequency coaxial amplitudes.

Flight	Line	Anomaly	Cat.	Inphase (ppm)	Quadrature (ppm)	Cond. (mhos)	Depth (metres)	EM bird ht. (metres)	UTM Easting (metres)	UTM Northing (metres)
17	10770	T	1	31	29.6	1.6	0	52	358444	6806211
17	10770	U	0	14.8	34.2	0.3	0	40	358289	6806040
17	10780	A	2	53.7	35.2	3.1	0	46	358346	6806298
17	10780	B	2	47.4	30.2	3.1	0	35	358403	6806365
17	10780	C	2	27.4	17.3	2.6	9	34	358624	6806624
17	10780	D	1	49.2	63.4	1.3	0	26	358830	6806866
17	10780	E	0	16	26	0.6	0	49	359092	6807181
17	10780	F	1	22.7	28.7	1	10	25	359440	6807522
17	10780	G	0	21.2	36.6	0.6	5	25	359480	6807559
17	10780	H	0	11	16.8	0.5	6	35	359555	6807665
17	10780	J	0	12.3	23.8	0.4	1	33	359617	6807745
17	10780	K	0	15.4	18.4	0.9	15	26	360050	6808208
17	10780	M	1	23.4	24	1.3	10	28	360142	6808335
17	10780	N	1	38	38.8	1.6	0	39	360205	6808404
17	10780	O	1	36.4	33.5	1.8	0	45	360233	6808434
17	10780	P	1	32.8	33.1	1.5	0	45	360333	6808598
17	10780	Q	1	32	28.4	1.8	0	45	360371	6808640
17	10780	R	1	30.9	29.8	1.6	0	50	360503	6808754
17	10780	S	0	17.9	50.3	0.3	0	37	360544	6808802
17	10780	T	2	21.7	10.1	3.7	0	51	360698	6809025
17	10780	U	2	14.1	6.3	3.4	0	75	360740	6809081
17	10790	A	3	71.6	34.5	5.1	0	32	360470	6808970
17	10790	B	2	53.6	35.5	3.1	1	32	360449	6808948
17	10790	C	2	39.3	28	2.5	0	50	360351	6808856
17	10790	D	0	19.7	25.9	0.9	0	42	360251	6808752
17	10790	E	0	10.8	11.6	0.9	15	34	360081	6808574
17	10790	F	3	77.4	37.3	5.3	0	46	359939	6808422
17	10790	G	0	12.5	21.6	0.5	0	47	359344	6807720
17	10790	H	1	19.2	20.4	1.1	0	56	359259	6807612
17	10790	J	1	18.2	17.7	1.3	0	59	358608	6806921
17	10790	K	2	39	28.8	2.4	0	57	358221	6806505
17	10790	M	2	30.2	22.5	2.2	0	61	358160	6806452
17	10800	A	2	47	25.4	3.9	0	53	357936	6806421
17	10800	B	2	56.4	40.1	2.9	0	47	358055	6806543
17	10800	C	2	70.3	66	2.2	0	34	358110	6806622
17	10800	D	1	45	46.7	1.6	0	30	358155	6806686
17	10800	E	1	92.4	112.7	1.7	8	13	358390	6806961
17	10800	F	1	49	70.1	1.1	8	17	358473	6807047
17	10800	G	0	9.6	35.5	0.1	9	15	358594	6807203
17	10800	H	1	40.3	38.7	1.7	0	47	358777	6807421
17	10800	J	2	84.9	88.3	2	0	32	358896	6807580
17	10800	K	2	90.1	68.3	3.1	0	37	358962	6807644
17	10800	M	0	12.2	25	0.4	0	40	359152	6807840
17	10800	N	0	12.2	25	0.4	0	40	359152	6807840
17	10800	O	0	6.5	13.9	0.2	0	42	359329	6808028
17	10800	P	0	6.5	13.9	0.2	0	42	359329	6808028

Anomaly parameters are calculated from the response of a vertical conductive half-plane in free using the mid-frequency coaxial amplitudes.

APPENDIX 4

STATEMENT OF QUALIFICATIONS

I, Bob B.H. Lo, am a Consulting Geophysicist with BHL Earth Sciences at 28 Nottinghill Road, Markham, Ontario, Canada, L3T 4X9. At the time of the data collection, I was the Chief Geophysicist of Aerodat Inc.

I graduated from the University of Toronto with a Bachelor of Applied Science degree in the Geophysics option of Engineering Science in 1981 and obtained a Masters of Science degree in Physics, also from the University of Toronto in 1985. In 1992, I obtained a Masters of Business Administration degree from Laurentian University in Sudbury, Ontario.

I am a member in good standing of the Professional Engineers of Ontario.

I am a member in the Society of Exploration Geophysicists—SEG (Tulsa), a member of the Canadian Exploration Geophysical Society—KEGS (Toronto), a founding member of the Environmental and Engineering Geophysical Society—EEGS (Denver), and a member of the Prospectors and Developers Association of Canada—PDAC (Toronto).

Since 1981, I have been involved in the use of geophysics for mineral exploration, geothermal site detection, and various engineering and environmental applications. I have either planned, supervised, conducted, interpreted, and reported on geophysical surveys from Canada, the United States of America, South America, South East Asia, Europe and Africa.

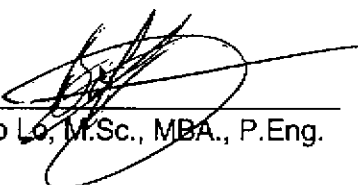
The statements contained in this report and the conclusions reached are based upon evaluation and review of maps and information supplied by Aerodat Inc., High-Sense Geophysics, and Pathfinder Minerals.

I have not visited the property nor hold any financial interest in the property.

Signed,

J9795
Markham, Ontario

March 3, 1998



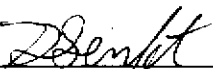
Bob Lo, M.Sc., MBA., P.Eng.

STATEMENT OF QUALIFICATIONS

I, Darren A. Senft, of #4-2415 W. 4th Ave., Vancouver, B.C. hereby declare that I:

1. Graduated from The University of British Columbia, Vancouver, B.C. with a B.Sc. in Geology in May, 1994.
2. Have been actively engaged in mineral exploration in Western Canada as a geological assistant with Cominco Ltd during the summers of 1992-94, as a contract geologist with Cominco Ltd from May, 1995 to May 1997, and as a permanent geologist with Cominco Ltd since May, 1997.

Date: March, 98

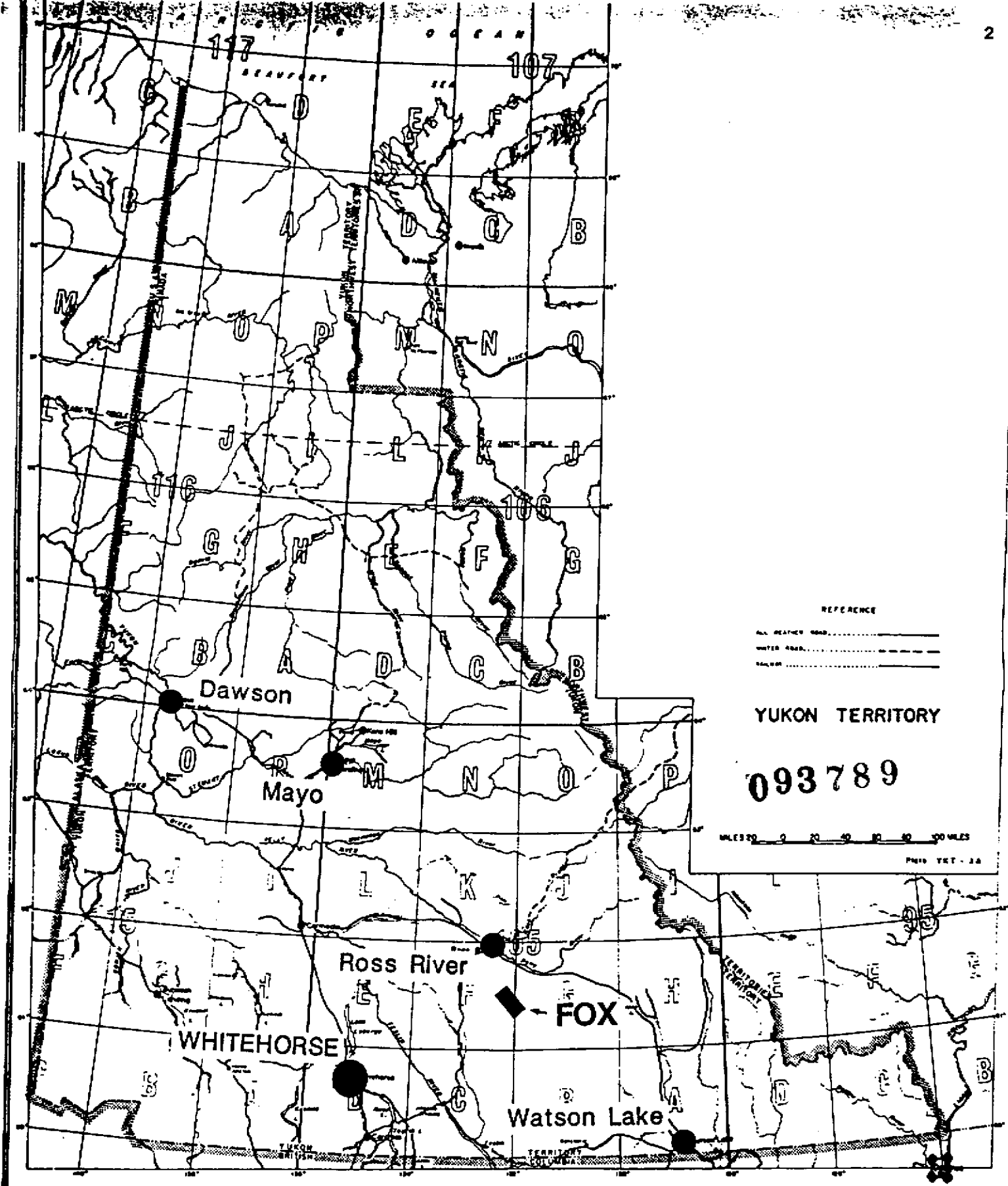


D.A. SENFT, B.Sc.
GEOLOGIST I

APPENDIX 5

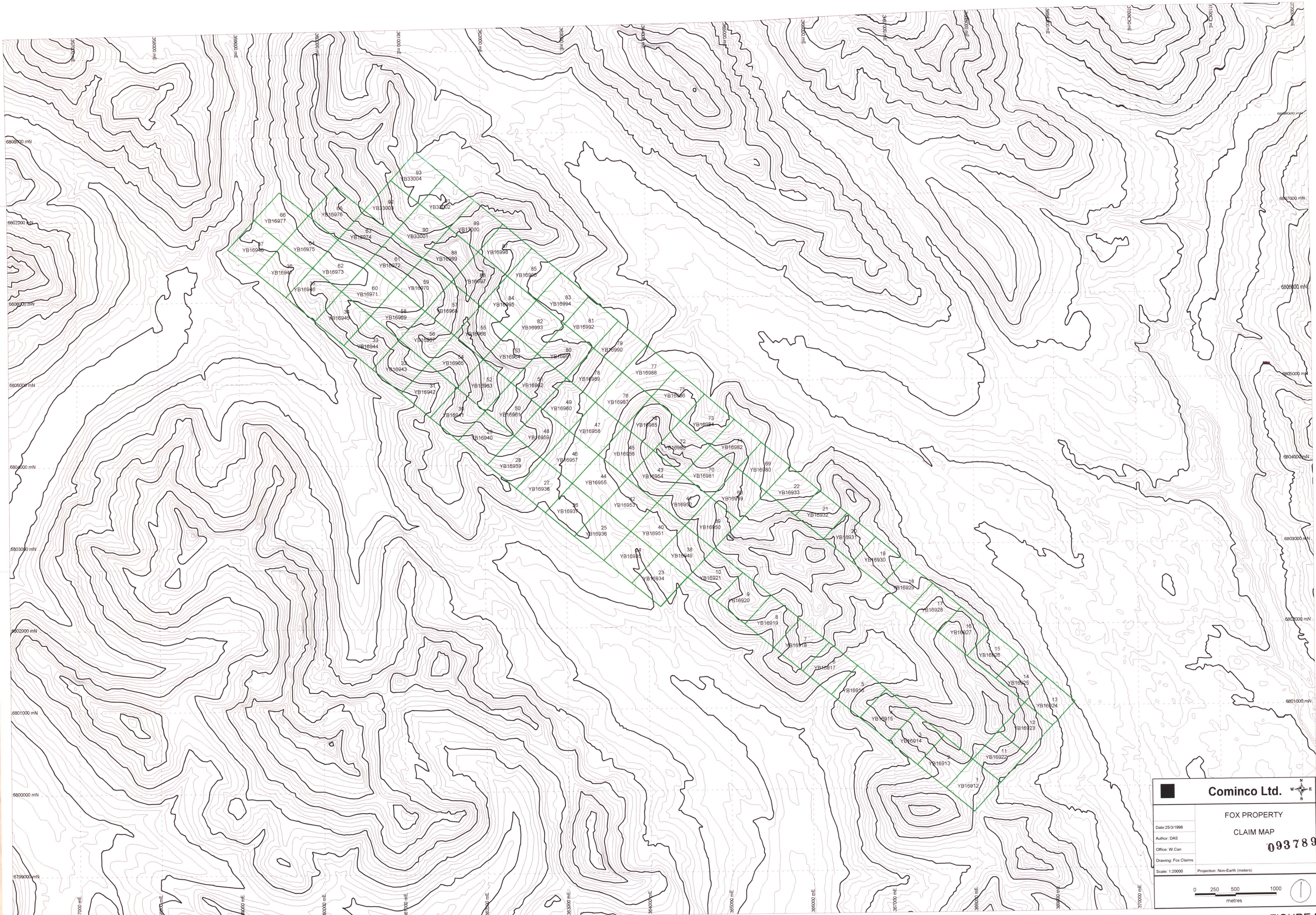
STATEMENT OF EXPENDITURES

Airborne EM/MAG Survey (160 line kms)	\$16,286.25
Cominco Staff Time	\$ 4,000.00
TOTAL	\$20,286.25



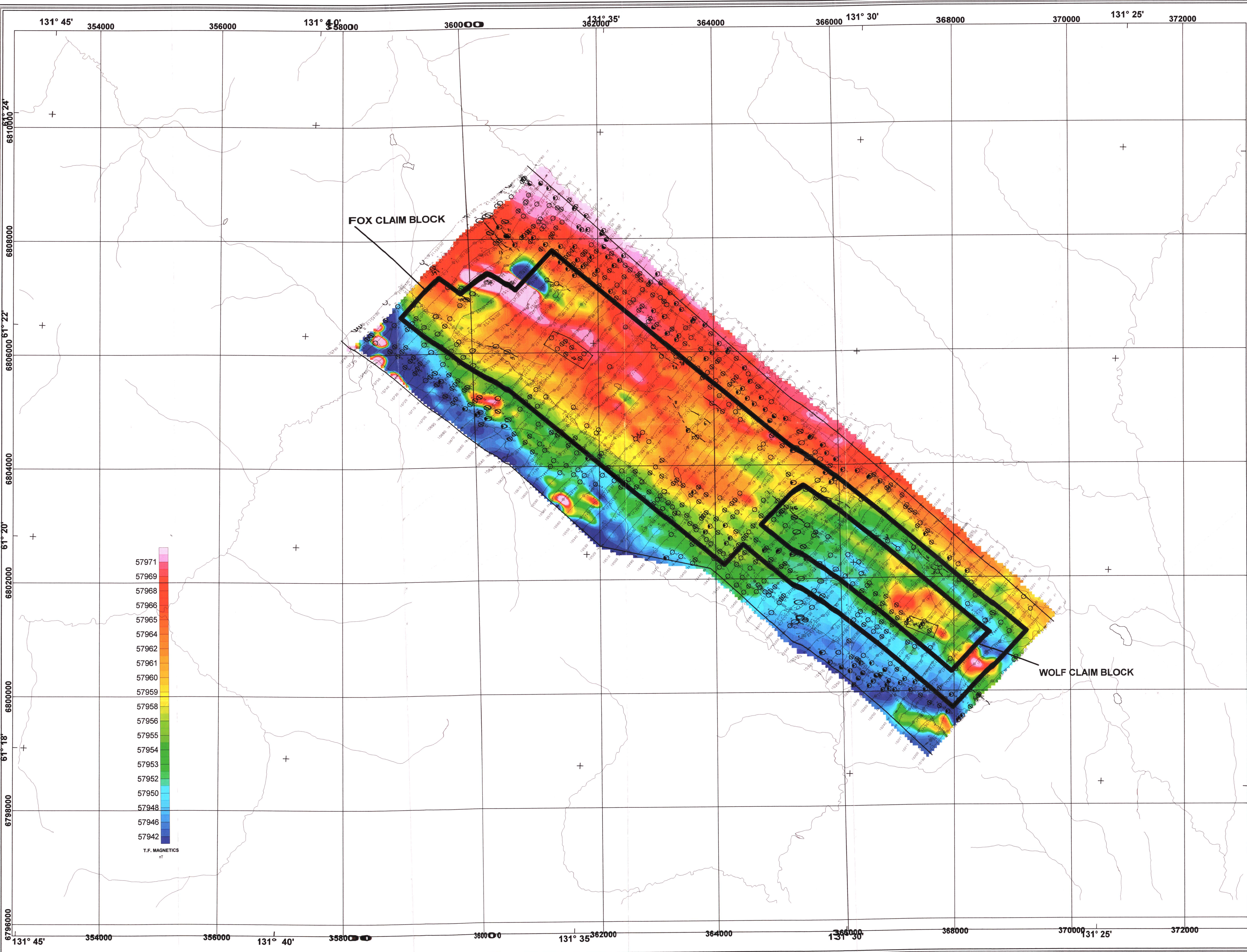
Drawn by:		Traced by:	
Revised by:	Date:	Revised by:	Date:

LOCATION MAP



Cominco Ltd.		
FOX PROPERTY CLAIM MAP 093789		
Date: 25/3/1998	Author: DAS	
Office: W. Can	Drawing: Fox Claims	
Scale: 1:20000	Projection: Non-Earth (meters)	

FIGURE 2



FLIGHT PATH

North American Datum 1927
 Clarke 1866 Ellipsoid
 Local transformation: dx=10, dy=158, dz=187
 UTM Projection
 Central meridian: 129°W
 Navigation and flight path recovery was conducted using a Global Positioning System (GPS) satellite navigation system.

Lines were flown at an azimuth of 40°-220°, with an average line spacing of 200 m.

Average helicopter-terrain clearance of 60 m was monitored by radar and barometric altimeters.

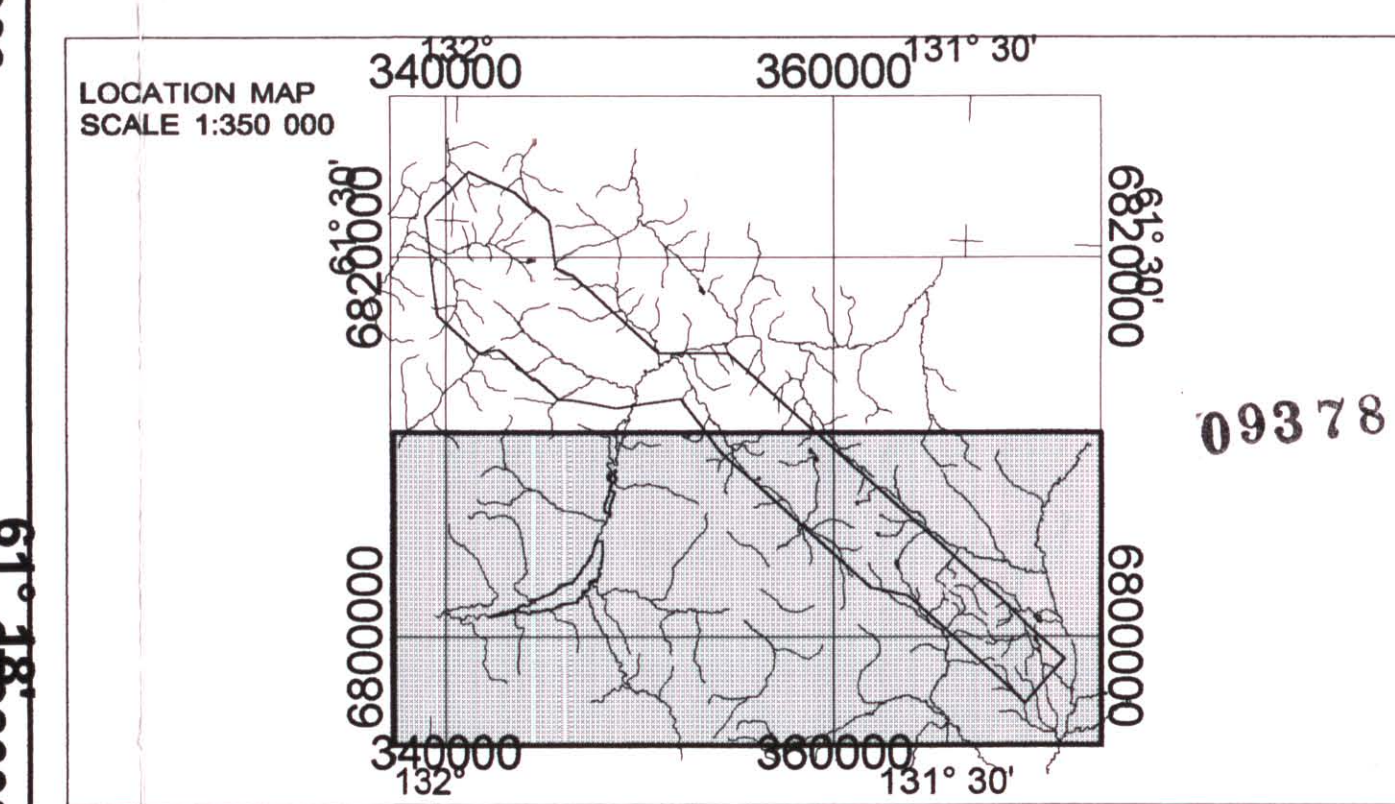
EM ANOMALIES

EM anomalies selected by computer algorithm and manually confirmed. Selection is based on the response correlation to theoretical sources such as steeply dipping conductors.

Calculation of conductance is based on the response of a vertical half plane conductor which is normal to the flight lines, using the 4365 Hz coaxial data.

Letter codes are used to identify individual anomalies on a line, and the inphase amplitude of the 4365 Hz response is annotated opposite.

- A 0-1 mhos
- B 1-2 mhos
- C 2-4 mhos
- D 4-8 mhos
- E 8-16 mhos
- F 16-32 mhos
- G >32 mhos
- M Magnetic



COMINCO EXPLORATION
 FINLAYSON LAKE AREA
 SOUTHERN YUKON

**EM INTERPRETATION
 And TOTAL FIELD MAGNETICS**

Scale 1:20,000

Map Scale: 1:20,000	Project Ref: J97-95
Date Compiled: Dec. 1997-Jan. 1998	Date Flown: Oct.-Nov. 1997

aerodat
 World Leader in Airborne Geophysics

FIGURE 3